

## Chapter 2

# Materials and Methods

Four major experimental sets have been performed using 413 rats to study the effect(s) of:

1. *Mild* indirect stimulation of the trigeminal afferents (by clipping of the contralateral vibrissal hairs)
2. *Intensive* indirect stimulation of the trigeminal afferents (by excision of the contralateral infraorbital nerve)
3. *Mild* direct stimulation of the vibrissal muscles (by massage)
4. *Intensive* direct stimulation of the vibrissal muscles (by electric current)

All animals were young adult (175–200 g) female Wistar rats (strain HsdCpb:WU, Harlan Winkelmann, Borcheln, Germany). They were fed standard laboratory food (Ssniff, Soest, Germany), provided with tap water *ad libitum*, and kept on a 12-h light–dark cycle. Experiments were conducted in accordance with the German law on the protection of animals; procedures were approved by the local animal care committee. We used only female rats because testosterone has been shown to beneficially affect peripheral nerve regeneration (Yu and Yu 1983).

### 2.1 First Major Set: Mild Indirect Stimulation of the Trigeminal Afferents After Combined Surgery on the Infraorbital and Facial Nerves by Removal (Clipping) of the Contralateral Vibrissal Hairs

#### 2.1.1 *Animal Groups and Overview of the Specific Methods Used in the First Experimental Set*

Forty-eight rats were randomly divided into four groups (Table 2.1).

Each group consisted of 12 rats that were subjected to unilateral combined injury (transection and suture, i.e., anastomosis) of the right facial (FFA) and infraorbital

**Table 2.1** Experimental design chart depicting animal grouping and procedures

Group of animals	Video-based motion analysis of vibrissae motor performance	Reinnervation pattern of motor end plates in m. levator labii superioris	Synaptic input to the facial motoneurons	Number of retrogradely labeled trigeminal ganglion cells
1. FFA + ION-S only	12	6	6	6
2. FFA + ION-S + VS	12	6	6	6
3. FFA + ION-S + MS	12	6	6	6
4. FFA + ION-S + VS + MS	12	6	6	6

FFA and ION-S indicate transection and end-to-end suture of the facial and infraorbital branch of the trigeminal nerves, respectively. VS = trimming of contralateral vibrissae to maximize ipsilateral vibrissal use for 4 months; MS = manual stimulation for 4 months; VS/MS indicates 2 months of VS followed by 2 months of MS. All 12 animals in each group underwent video-based motion analysis of the vibrissae motor performance. Thereafter, half of the animals were used to study the reinnervation pattern of m. levator labii superioris. The other six rats in each group were used for retrograde labeling of the facial and trigeminal neurons in the brainstem

(ION-Suture, ION-S) nerves. Rats from group 1 underwent surgery, but received no postoperative therapy (FFA + ION-S-only), whereas rats from groups 2–4 were used to assess the efficacy of three treatment paradigms:

1. Removal of the contralateral vibrissae to ensure a maximal use of the ipsilateral ones (vibrissal stimulation; FFA + ION-S + VS; group 2)
2. Manual stimulation of the ipsilateral vibrissal muscles (FFA + ION-S + MS; group 3)
3. Vibrissal stimulation followed by manual stimulation (FFA + ION-S + VS + MS; group 4)

No intact controls were included in this major experimental set because our aim was not to compare functional and morphological parameters between surgically treated and intact animals: It is well known that after peripheral nerve injury, recovery of function is poor and never reaches levels comparable to those in intact animals.

Four months after combined surgery, all rats were videotaped to determine vibrissal motor performance during explorative whisking using motion analysis system (Table 2.2).

Thereafter, one half of the animals in each group were used to determine the proportion of mono- and polyinnervated motor end plates (Table 2.3) in the ipsilateral levator labii superioris muscle by means of immunocytochemistry for neuronal class III  $\beta$ -tubulin and histochemistry with  $\alpha$ -bungarotoxin (see below).

The animals from the second half were used to establish changes in the synaptic input to the facial motoneurons that projected to the whisker pad muscles (identified by retrograde labeling with FB, Table 2.4) and to document eventual changes in the number of those trigeminal ganglion cells sending their dendrites into the infraorbital nerve.

**Table 2.2** Motor recovery after combined facial and trigeminal nerve injury and stimulations

Group of animals	Frequency (in Hz)	Angle at maximal protraction (in degrees)	Amplitude (in degrees)	Angular velocity during protraction (in degrees/s)
1. FFA + ION-S only	6.2 ± 1.0	98.0 ± 8.0	11 ± 4.0	138 ± 37
2. FFA + ION-S + VS	6.4 ± 1.5	77.0 ± 11 <sup>a</sup>	28 ± 9.0 <sup>a</sup>	439 ± 113 <sup>a</sup>
3. FFA + ION-S + MS	6.0 ± 1.0	76.0 ± 9.0 <sup>a</sup>	30 ± 11 <sup>a</sup>	497 ± 163 <sup>a</sup>
4. FFA + ION-S + VS + MS	6.3 ± 1.0	74.0 ± 8.0 <sup>a</sup>	32 ± 10 <sup>a</sup>	528 ± 107 <sup>a</sup>

Biometrics of vibrissae motor performance in rats after transection and suture of the right facial and infraorbital nerves (*FFA + ION-S only*), in rats subjected to FFA + ION-S and postoperative clipping of the contralateral vibrissal hairs, that is, vibrissal stimulation (*FFA + ION-S + VS*), in rats subjected to FFA + ION-S and postoperative mechanical stimulation of the vibrissal muscles (*FFA + ION-S + MS*), and in rats subjected to FFA + ION-S and postoperative vibrissal and mechanical stimulations (*FFA + ION-S + VS + MS*). All groups consisted of 12 animals. Shown are group mean values ± SD. Significant differences between group mean values (ANOVA and post hoc Tukey's test,  $p < 0.05$ )

<sup>a</sup>From FFA + ION-S only

Values adapted from Bendella et al. (2011)

**Table 2.3** Quality of target muscle reinnervation

Group of animals	Monoinnervated motor end plates (percent)	Polyinnervated motor end plates (percent)	Non-innervated motor end plates (percent)	Total number of motor end plates examined
1. FFA + ION-S only	35 ± 7.6	58 ± 8.3	7.3 ± 1.4	1,461 ± 241
2. FFA + ION-S + VS	52 ± 7.1 <sup>a</sup>	40 ± 3.4 <sup>a</sup>	8.1 ± 2.2	1,509 ± 235
3. FFA + ION-S + MS	53 ± 6.1 <sup>a</sup>	40 ± 4.1 <sup>a</sup>	7.2 ± 3.1	1,719 ± 143
4. FFA + ION-S + VS + MS	56 ± 3.1 <sup>a</sup>	33 ± 10 <sup>a</sup>	11 ± 3.6	1,482 ± 332

Innervation patterns of the m. levator labii superioris (LLS) motor end plates. Values are means ± SD,  $n = 6$  per group

<sup>a</sup>Differences between animals receiving no treatment (group 1) and those receiving VS, MS or VS/MS (ANOVA and post hoc Tukey's test,  $p < 0.05$ )

All abbreviations are as in Table 2.1

### 2.1.2 Combined Nerve Surgery (*FFA + ION-S*)

All surgery was unilateral and performed on the right side under surgical anesthesia (ketamine/xylazine, 100 mg Ketanest<sup>®</sup>, Parke–Davis/Pfizer, Karlsruhe, Germany, and 5 mg Rompun<sup>®</sup>, Bayer, Leverkusen, Germany, per kg body weight; i.p.).

*Facial–Facial Anastomosis (FFA)*. The facial nerve was exposed, transected close to its emergence from the stylomastoid foramen, and sutured end to end with two 11–0 atraumatic sutures (Ethicon, Norderstedt, Germany) (Fig. 2.1a).

*Transection and Suture of the Infraorbital Nerve (ION-Suture, ION-S)*. The infraorbital branch (infraorbital nerve, ION) of the ipsilateral trigeminal nerve was exposed at its exit from the infraorbital foramen. All its 4–6 peripheral fascicles were

**Table 2.4** Synaptic input to the facial nucleus as estimated by means of widefield fluorescence microscopy (WFM) and confocal laser scanning microscopy (CLSM)

Group of animals	Widefield		Fluorescence		Microscopy		Confocal		Microscopy	
	Synaptophysin containing fraction area in percentage		Number of synapses per motoneuron		Synaptic density (per mm)		Number of synapses per motoneuron		Synaptic density (per mm)	
1. FFA + ION-S only	11.84 ± 1.45		16.48 ± 7.05		128.53 ± 35.04		21.19 ± 6.03		124.80 ± 13.21	
2. FFA + ION-S + VS	11.76 ± 1.38		16.15 ± 6.75		126.34 ± 35.63		22.11 ± 5.52		128.08 ± 12.92	
3. FFA + ION-S + MS	12.75 ± 1.96		16.52 ± 6.29		133.70 ± 40.96		25.12 ± 4.02		132.61 ± 16.96	
4. FFA + ION-S + VS + MS	11.47 ± 1.77		16.39 ± 7.10		128.58 ± 36.23		23.49 ± 5.10		127.64 ± 16.16	

Counts of synapse number and density within the borders of selected RoIs. Values are means ± SD,  $n = 6$  per group. There were no differences between rats receiving no intervention and those receiving VS, MS, or VS/MS (ANOVA and post hoc Tukey's test,  $p < 0.05$ ). All abbreviations are as in Table 2.1

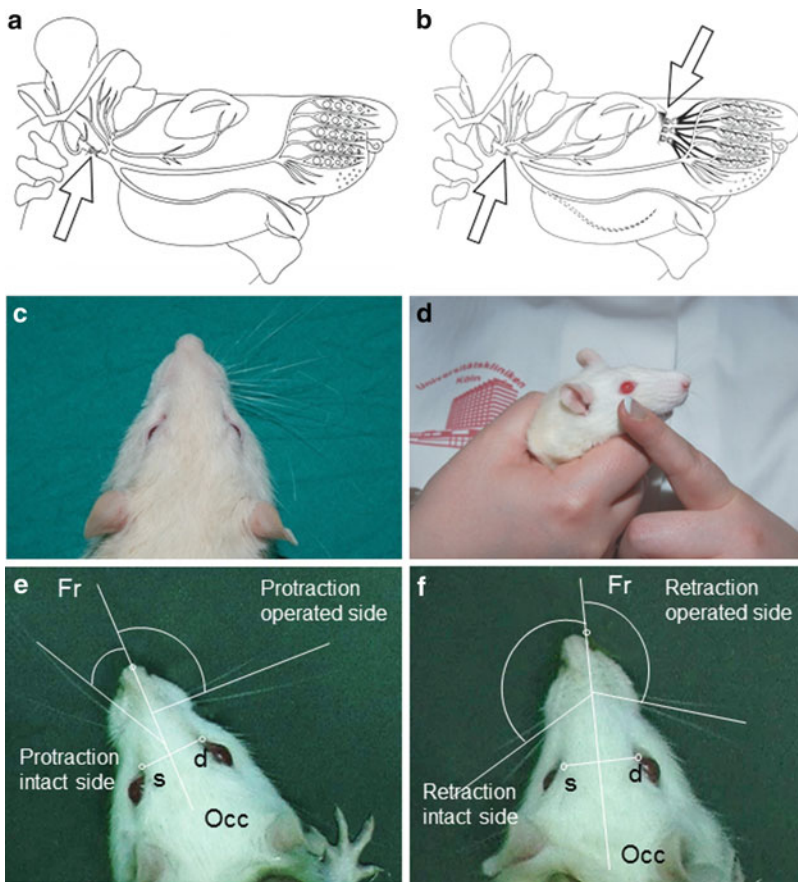


**Fig. 2.1** (a, b) Schematic drawings illustrating transection and end-to-end suture of the infratemporal portion of the facial nerve (a, arrow) and the infraorbital branch of the trigeminal nerve (b, upper arrow). Adapted from (Dörfl 1985; Semba and Egger 1986). (c, d) Postoperative treatments. The vibrissae on the left side of the face are trimmed to maximize vibrissal use on the operated, right, side (c). Manual stimulation of the whisker pad skin and musculature on the operated, right, side (d). The developed spatial model allows precise measurement of angles, angular velocity, and angular acceleration on the intact (left) and operated side (right) during protraction (e) and retraction (f) of the vibrissae. Note the significant change in angle between the sagittal line **Fr-Occ** during protraction and retraction on the intact side. The vibrissae on the operated side remain paretic. Adapted from Tomov et al. (2002)

transected and sutured sequentially one by one (Fig. 2.1b). Theoretically, unilateral lesioning of the infraorbital nerve (ION) could by itself damage ipsilateral vibrissal motor function: The vibrissal system is a sensory–motor loop closed on several levels within sensorimotor structures of the nervous system (Erzurumlu and Killackey 1979; Kleinfeld et al. 1999; Nguyen and Kleinfeld 2005). However, elegant earlier work has shown that profound changes that follow ION injury are not mirrored by the amount of vibrissal muscle motor innervation and function even in newborn rats which are highly sensitive (Veronesi et al. 2006).

### ***2.1.3 Increased Ipsilateral Vibrissal Use (Vibrissal Stimulation, VS) After Combined Surgery in Group 2***

On the day following surgery, animals in group 4 (FFA + ION-S + VS) had the contralateral vibrissae clipped (Fig. 2.1c) under light narcosis (Isofluran, O<sub>2</sub> and Nontix: N<sub>2</sub>O; Linde AG, Pullach, Germany). Clipping was repeated every third day for 4 months. In this way we hoped to maximize the use of the ipsilateral vibrissae (VS) and therefore to achieve a sensory stimulation of the vibrissal afferent system (Staiger et al. 2000; Hoffman et al. 2003; Machin et al. 2006).

Theoretically, unilateral vibrissae clipping might also trigger an artificially retracted position of the head on the opposite side (Hadlock et al. 2008; Heaton et al. 2008). This phenomenon is observed regularly in all animals that undergo facial nerve transection. Since rats cannot move the vibrissae on the side of the transection (usually the right nerve), they move their heads in a manner allowing maximum exploration with the intact left vibrissae; this leads to a deviation of the head toward the right shoulder. We did not observe increased deviation of the head in animals subjected to trimming of the vibrissae.

Despite clipping of the left whiskers in group 4, our approach should be sharply differentiated from bilateral removal of sensory input: the trigeminal afferents on the side contralateral to FFA are intact and despite clipping 0.5–1.0 mm hair length always remained. Accordingly, animals did not show overt signs of stress, for example, freezing, biting, weight loss, or lack of grooming.

Other possible consequence of depriving animals of normal sensory input on one side of the face is a vigorous whisking on the opposite side. However, we did not observe abnormal use of ipsilateral vibrissae following contralateral clipping, although we watched the animals carefully throughout the entire postoperative period. Rather, animals quickly became accustomed and explored their environment in a manner such that they maximized the likelihood of interactions with objects in their environment while ensuring that such interactions involved only gentle touch (Mitchinson et al. 2007). Thus, the probability to observe a hyperfunction of the contralateral motor facial system, due to abnormally intensive use of the vibrissal hairs, was minimal, and we did not include a separate group of animals with intact facial and trigeminal nerves that had been subjected to enhanced vibrissal stimulation (VS). Since animals could only be videotaped if they had sufficiently long vibrissal hairs on both sides of the face, rats in group 4 were allowed to survive 1 week longer than those in the other groups.

### ***2.1.4 Manual Stimulation of Vibrissal Muscles After Combined Surgery in Groups 3 and 4***

In group 3 (FFA + ION-S + MS), MS was initiated on the day following surgery, and in group 4, MS was initiated after 2 months of VS. The right whisker pad (vibrissal hairs, fur, nerves, blood vessels, and vibrissal muscles) were gently and rhythmically stroked by hand for 5 min per day for 5 days a week (Fig. 2.1d) as previously described (Angelov et al. 2007).

### ***2.1.5 Observations on Whisking Behavior***

Before each manual stimulation and clipping of the left vibrissae, rats were carefully observed (for about 3–5 min) over the entire course of the experiment.

### ***2.1.6 Analysis of Vibrissae Motor Performance During Exploration***

Video-based motion analysis of explorative vibrissal motor performance was performed as described previously in rats (Guntinas-Lichius et al. 2002, 2005b; Tomov et al. 2002) and in mice (Angelov et al. 2003; Guntinas-Lichius et al. 2005a).

The key movements of the vibrissae are protraction (Fig. 2.1e) and retraction (Fig. 2.1f). Since all vibrissal piloerector muscles are innervated by the buccal branch (Dörfl 1985), the whiskers acquire caudal orientation and remain motionless following transection of the facial nerve. Two large vibrissae of the C-row, that is, the third row from dorsal [see Fig. 1 in Arvidsson (1982) and Fig. 2.12b)], on each side of the face were used for biometric analysis, as described previously (Guntinas-Lichius et al. 2001). Under light anesthesia, all other vibrissae were clipped using small fine scissors, and the animals were inserted into a rodent restrainer (Hugo Sachs Elektronik—Harvard Apparatus GmbH, 79232 March-Hugstetten, AH 52–0292) for 30 min to pacify them. Employing a digital camcorder (Panasonic NV-DX 110 EG), animals were videotaped for 3–5 min during active exploration. After calibration, video images of whisking behavior were sampled at 50 Hz (50 fields per second); the video camera shutter opened for 4 ms. Images were recorded on AY-DVM 60 EK mini cassettes. Captured video sequences were reviewed and 1.5-s sequence fragments from each animal selected for analysis of whisking biometrics. Thereby, the stable position of animal's head, the frequency of whisking, and the degree of vibrissae protraction were considered as selection criteria.

The tip of the rat's nose and the inner angles of both eyes were defined as reference points. Each vibrissa in the spatial model was represented by 2 points—its base and a point on the shaft 0.5 cm away from the base. Using this model, the following parameters were evaluated: (1) protraction (i.e., the forward movement of the vibrissae) measured by the rostrally opened angle (in degrees) between the midsagittal plane and the hair shaft, (2) the whisking frequency as cycles of protraction and retraction (passive backward movement) per second, (3) the amplitude (the difference between maximal retraction and maximal protraction in degrees), (4) the angular velocity during protraction in degrees per second, and (5) the angular acceleration during protraction in degrees per square second. Measurements were performed by three observers (S.K. Angelova, D. Bösel, D. Felder) who were blinded as to the treatments of the rats.

To clarify the terminology, rodents make a number of different movements with their whiskers, namely, (1) large-amplitude “explorative” sweeps of the vibrissae (in the frequency range of 5–11 Hz), (2) low-amplitude “foveal” or “palpating” whisker movements (at 15–25 Hz; Semba et al. 1980; Berg and Kleinfeld 2003), and (3) denervation-induced tremor that occurs after facial nerve transection (Semba and Komisaruk 1984). All whisker movements are elicited by contractions of the intrinsic and extrinsic vibrissal musculature which are controlled solely by the facial nerve (Dörfl 1985). In this study, we analyzed only the large-amplitude exploratory sweeps. Following facial nerve transection, such exploratory movements are completely abolished. However, with time, and as we show here, there is a gradual progression to varying levels of motor performance which can be readily assessed by video-based motion analysis. The technique is an entirely noninvasive approach to monitor recovery of function after facial nerve repair and avoids the use of invasive electromyography.

### **2.1.7 Fixation**

*Fixation.* At the end of the designated postoperative survival time, all rats were transcardially perfused with 0.9 % NaCl in distilled water for 60 s followed by a fixation with 4 % paraformaldehyde in 0.1 M phosphate buffer (pH 7.4) for 20 min under deep anesthesia.

### **2.1.8 Analysis of Target Muscle Reinnervation**

Determination of the ratio between mono- and polyinnervated motor end plates was performed as described previously (Guntinas-Lichius et al. 2005b). The levator labii superioris muscles (Fig. 2.2a) were dissected free, cryoprotected in sucrose, and cut longitudinally (30  $\mu$ m) on a cryostat. Sections were immunostained with a rabbit polyclonal antibody against neuronal class III  $\beta$ -tubulin (Covance, Richmond, CA, USA, No. PRB-435P, 1:1,000) and Cy3-conjugated anti-rabbit IgG (1:400; Sigma). Subsequently, motor end plates were stained with Alexa Fluor 488-conjugated  $\alpha$ -bungarotoxin (Molecular Probes, 1:1,000). Quality of end plate reinnervation was evaluated by a simple and straightforward criterion, that is, the number of axonal branches (identified by beta-tubulin staining) that enter or, in some cases, possibly leave the boundaries of individual end plates (identified by acetylcholine receptor staining with alpha-bungarotoxin). Entries by preterminal branches of one axon were counted as single events. According to this criterion, the end plates were identified as “monoinnervated” (one axon; Fig. 2.2c), “polyinnervated” (two or more axons; Fig. 2.2b), or denervated (no visible axonal associated with the receptor staining). The term “polyinnervated end plates” is used to indicate similarity to a morphological abnormality in adult skeletal muscle of mammals observed in pathological conditions such as nerve damage or intoxication that cause axonal branching, which is either

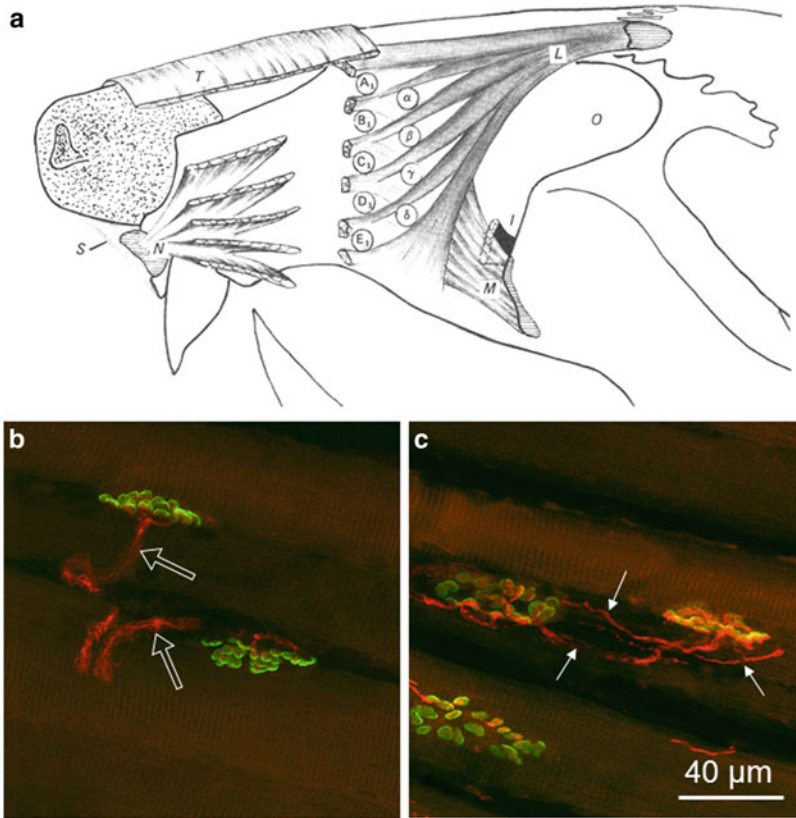


**Fig. 2.2** (a) Schematic drawing of the extrinsic vibrissae muscles according to Dörfel (1982):  $\alpha$ - $\delta$ : the four caudal hair follicles, the muscles slings of which “straddle” the five vibrissae rows (A–E); T—m. transversus nasi; L—m. levator labii superioris; N—m. nasalis; M—m. maxilolabialis; O—orbit; S—septum intermusculare. (b, c) Superimposed stacks of confocal images of end plates in the levator labii superioris muscles of intact and surgically treated rats visualized by staining of the motor end plates with Alexa Fluor 488  $\alpha$ -bungarotoxin (green fluorescence) and immunostaining of the intramuscular axons for neuronal class III  $\beta$ -tubulin (Cy3 red fluorescence). (c) and (b) show examples of a polyinnervated and a mono-innervated end plate, respectively. Three axonal branches (arrows in (c)) reach the boundaries of the polyinnervated end plate delineated by the alpha-bungarotoxin staining. In contrast, the mono-innervated end plates in (b) are reached by a single axon (empty arrows in (b)) with several preterminal rami. Adapted from Sinis et al. (2009)

collateral (at nodes of Ranvier) or terminal (from end plate terminals) or both (Rich and Lichtman 1989; Son et al. 1996). Under such conditions many individual end plates are innervated by more than one motoneuron, that is, they are “polyneuronally” innervated. We use the term “polyinnervated end plates” rather than the term “polyneuronally innervated end plates” to indicate that we have not identified the perikaryal origins of supernumerary axons in individual end plates, that is, we did not identify one or more parent motoneurons. Counts of end plates were performed directly under the microscope (objective  $\times 40$ ) in a blind fashion.

### 2.1.9 Synaptic Input to the Facial Motoneurons

Perikarya in the facial nucleus were visualized by bilateral retrograde labeling with Fast Blue (FB). Under deep ether anesthesia, 1 mg FB (in 100  $\mu$ l distilled water, 2 % dimethyl sulfoxide) was injected subcutaneously at the midpoint between the two dorsal vibrissae in rows A and B (Arvidsson 1982; Angelov et al. 1993; Angelov et al. 1994; Streppel et al. 1998; Popratiloff et al. 2001) (Fig. 2.3a). Tracer was injected at identical sites in each animal allowing for comparison of synapse numbers on retrogradely labeled perikarya. Sections through the trigeminal ganglia of the same animals were used to examine anatomical restoration of the ION (see below).

*Tissue Preparation and Immunocytochemistry.* Perfusion-fixed (4 % paraformaldehyde) brainstems were cut (coronal, 30  $\mu$ m) and every fifth section through the facial nucleus stained immunohistochemically in one incubation batch for all 24 rats. Sections were immunostained with anti-synaptophysin, an established pan-marker for presynaptic terminals, on a shaker at room temperature using (1) 5.0 % (w/v) bovine serum albumin (BSA, Sigma) in TBS for 30 min; (2) 1:4,000 anti-synaptophysin (rabbit polyclonal anti-synaptophysin, Biometra) in TBS plus 0.8 % (w/v) BSA for 2 h; (3) 5.0 % (v/v) normal sheep serum (NSS, Sigma) plus 0.8 % BSA in TBS for 15 min; and (5) anti-rabbit IgG Cy3 conjugate (1:400; Sigma) in TBS plus 0.8 % NSS for 1 h.

*Fluorescence Microscopy and Photography.* Using a slow-scan CCD camera (Spot RT3 Slider, Diagnostic Instruments, Inc., USA) on a Zeiss Axioplan microscope (Carl Zeiss, Jena, Germany; stabilized powerful UV source: XBO 75 W/HBO100W), images of the facial nucleus from the operated and unoperated side were captured (magnification  $\times 10$ ). We first photographed FB-labeled perikarya (“ultraviolet” filter set 01: excitation BP 365/12, emission LP 397; Carl Zeiss). Synaptic terminals, visualized in red by the CY3 fluorochrome, were then photographed (“rhodamine filter set 15: excitation BP 546/12, emission LP 590; Carl Zeiss). Exposure times were optimized to ensure saturation of only a few pixels. All images were captured under identical conditions. Both picture sets were taken in 14-bpp TIFF format and saved in 16-bpp TIFF format in which every pixel contains 16 bits encoding brightness, ranging from 0 to 65,536, with higher numbers indicating greater brightness (Fig. 2.3b–e).

*Image Analysis to Determine Synaptic Density Using Widefield Microscopy.* FB-images were used to define “regions of interest” (RoIs) in each picture of the facial nucleus (ImageJ Software v1.38, NIH, Bethesda, Maryland, USA) through the following steps: (1) The dynamic range of the FB-images was maximized using gamma correction ( $\gamma = 0.2$ ). (2) Images were sharpened by subtraction of a blurred copy (Gaussian blurring radius = 75px). (3) Images were automatically thresholded using the Otsu algorithm to produce binary black-and-white images. (4) Motoneurons were included by selecting only FB-labeled areas with a value equal or greater than 500  $\mu\text{m}^2$ . The resulting masks were used to measure the perimeter and area of the selected motoneurons. (5) The perimeters were drawn and expanded in and out by 2px which generated RoIs from the closest perisomatic vicinity of the

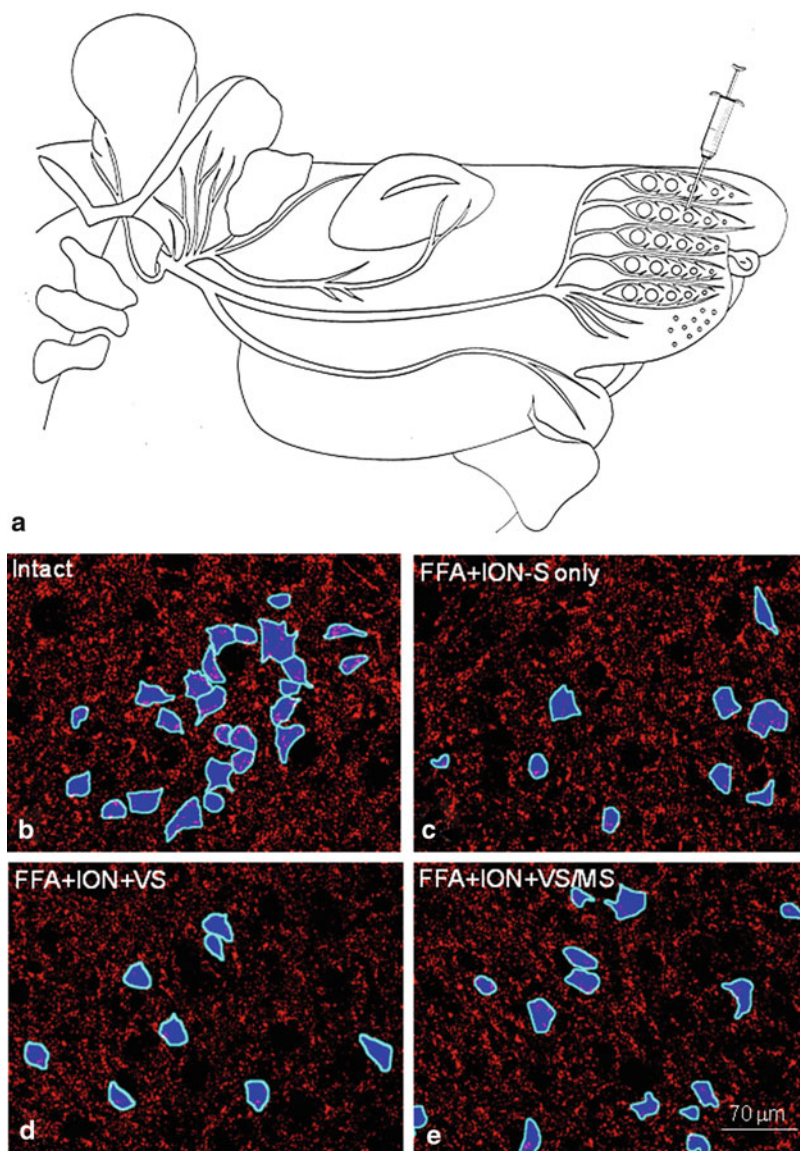


**Fig. 2.3** (a) Schematic drawing indicating the injection site of the retrograde tracer Fast Blue (syringe in (a)) into the whisker pad. (b–e) Retrogradely labeled motoneuronal perikarya (blue) and synaptophysin-CY3 immunostaining (red) of axosomatic nerve boutons in the intact facial nucleus (b) and 4 months after FFA + ION-S only (c), after FFA + ION + VS (d), and after FFA + ION + VS/MS (e) Scale bar indicates 70  $\mu\text{m}$

motoneurons with a width of 5px ( $\approx 4 \mu\text{m}$ ; Fig. 2.3b–e). All synaptophysin-positive profiles found within each of the predefined perisomatic RoIs of the thresholded images were counted and the “numbers of perisomatic synapses per motoneuron”

determined. To correct for size differences, these numbers were weighted with the corresponding perikaryal perimeters to calculate the “linear synaptic density,” that is, the number of synapses per mm (Table 2.4).

*Image Analysis to Determine the Synaptophysin-Positive Fraction Area in the Lateral Facial Subnucleus.* All synaptophysin-positive profiles were processed using a morphological filtering algorithm (top-hat opening by reconstruction), which was similar to the digital background subtraction via granulometric filtering (Prodanov et al. 2006): (1) To define the maximal and minimal radius of the positive profiles before processing, 50 randomly selected images from all experimental sets were subjected to granulometry (data not shown; Grayscale Granulometry for ImageJ, Prodanov D., 2003–2008, <http://www.diagnosticarea.com/plugins/gmplugins.html#gran>). (2) Next all images were filtered through a minimum filter, the radius of its “wholes” being equal to the minimal profile radius that was measured (6px). This procedure removed all profiles which were smaller than the filter radius. (3) Background was restored using morphological reconstruction (Landini G. GreyscaleReconstruct\_v.2.1. for ImageJ, available from <http://www.dentistry.bham.ac.uk/landinig/software>. Accessed on 08.07.2010). (4) Background images were subtracted from the originals, which produced images of all positive profiles smaller than the predefined maximal radius (6px). (5) The profile images were binarized by automatic thresholding via the Otsu algorithm. (6) To separate adjacent synaptophysin-positive particles, a “watershed” neighborhood operation was applied to the thresholded images (Fig. 2.4a–d).

To measure the synaptophysin immunoreactivity in the lateral facial subnucleus, all processed profiles were counted by the software, which provided also information on mean area and mean fraction area. This in turn allowed us to calculate the total area of immunopositive profiles as well as the relation of this total area to the area of a given image (particle covered area fraction).

At first glance these stringent features of the method are quite likely to impose substantive biases on the final absolute numbers (i.e., undercounting), mostly arising from the important cell- and synaptic bouton-volume dependence. This undercounting would, however, be the same in all four experimental groups. Furthermore, a quantification of the expression (e.g., intensity of fluorescence) of immune-related antigens by immunocytochemical methods in *absolute values* is considered fraught: The different antigens do not react equally well with the antibodies used (Neefjes and Ploegh 1992). In addition, antibody binding molecules have been observed in large invaginations of the tissue that are not accessible for the incubation medium (Harding et al. 1990). Thus, any quantification of immunopositive cells and cell processes should be considered *relative* and employed only for comparison. Anyway, in analogy to earlier work (Calhoun et al. 1996) we decided to repeat our observations in thin confocal optical sections and thus improve the identification of puncta around the FB-labeled motoneuronal perikarya.

*Quantification of Perisomatic Synaptophysin-Positive Puncta.* Estimations of perisomatic synaptophysin-positive puncta were performed as described previously (Irintchev et al. 2005). Immunostained sections through the facial nucleus were

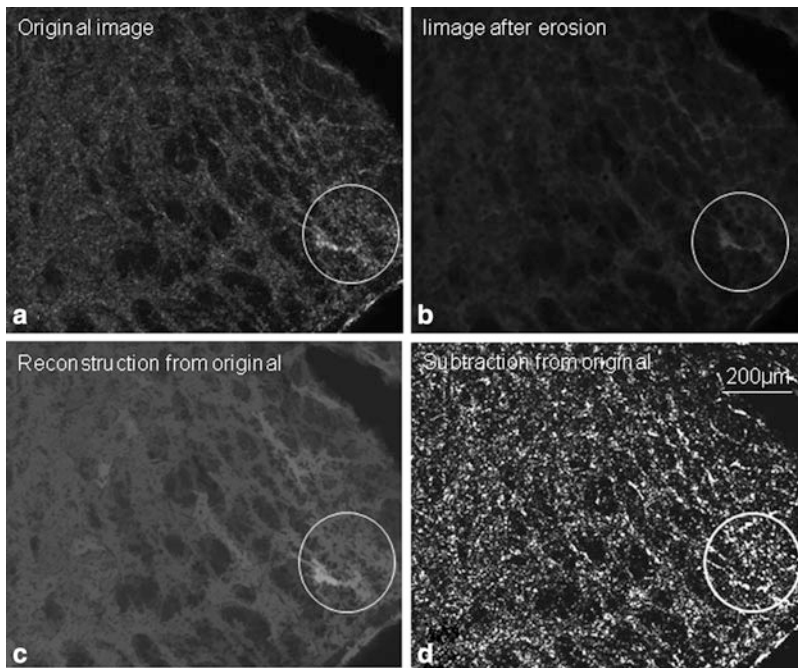


**Fig. 2.4** (a–d) Steps in image processing of widefield epifluorescence microscopy. (a) Original image; (b) Erosion of image (a) with “minimum filter” with radius 6px. All objects with radius 6px or less are removed and the image is heavily degraded; (c) Reconstruction of the eroded image (b) from the original (opening by reconstruction). The image is restored to the original state, but all objects with radius 6px or less are missing; (d) Subtraction of the reconstructed image from the original (top-hat opening by reconstruction). This operation isolates from the original unprocessed image only the objects with radius 6px or less. Scale bar indicates 200  $\mu\text{m}$

examined under a fluorescence microscope. Stacks of images of 1- $\mu\text{m}$  thickness were obtained on a TCS SP5 confocal microscope (Leica) using a 40  $\times$  oil immersion objective and digital resolution of 1,024  $\times$  1,024 pixels. Four adjacent stacks (frame size, 115  $\times$  115  $\mu\text{m}$ ) were obtained consecutively in a rostrocaudal direction so that more motoneurons could be sampled. One image per cell at the level of the largest cell body cross-sectional area was used to count the number of perisomatic puncta (see Fig. 2.5). Motoneurons were easily identified by the retrograde labeling with FB. Areas and perimeters were measured using the Image Tool 2.0 software program (University of Texas, San Antonio, TX, free software available at <http://ddsdx.uthscsa.edu/dig/>). Linear density was calculated as number of perisomatic puncta per unit length. Between 105 and 120 cells were analyzed for synaptic linear density per animal.

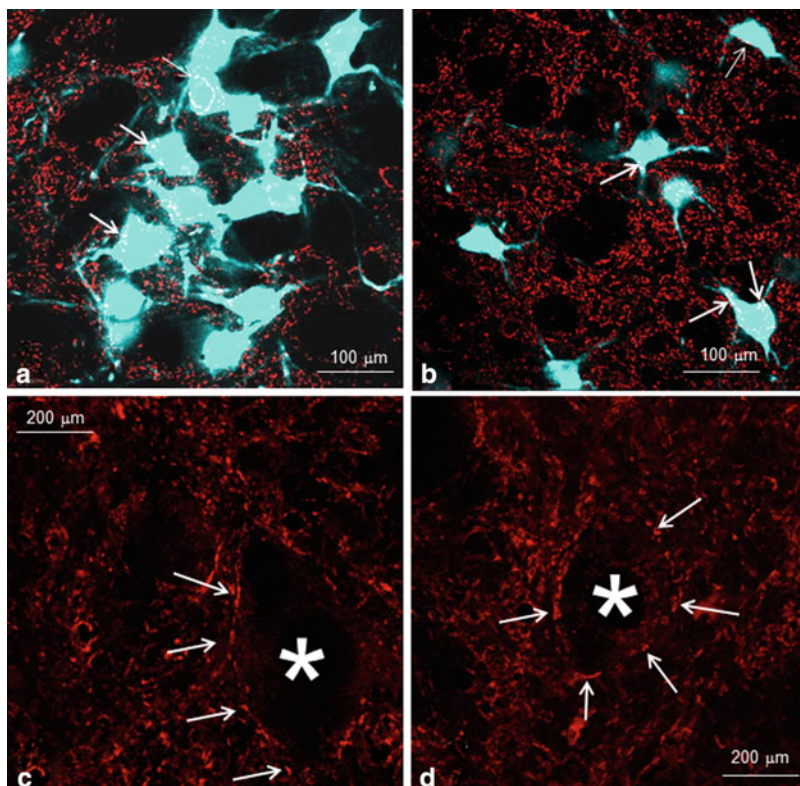


**Fig. 2.5** (a–d) Analysis of perisomatic synaptophysin-positive puncta. (a, b) Low-power confocal images (1- $\mu$ m-thick optical slices) show the appearance of synaptophysin-positive puncta (arrows) around intact (a) and axotomized (b) facial motoneurons identified by the retrograde labeling with FB. (c, d) High-power confocal images used for counting: intact (c) and axotomized (d) motoneuronal cell bodies (asterisks) 4 months after regeneration following facial and infraorbital nerve transaction and end-to-end suture. Scale bar in (a, b) indicates 100  $\mu$ m, in (c, d) 200  $\mu$ m

### 2.1.10 Number of Retrogradely Labeled Trigeminal Ganglion Cells

It is well known that trigeminal ganglion neuron numbers vary significantly with age between 3 and 8 months (Lagares et al. 2007), that is, exactly in the period in which we performed our experiments. Nevertheless, we decided to examine the extent of anatomical integrity in the trigeminal ganglion after transection and suture of the infraorbital nerve (ION) and compared the number of retrogradely labeled pseudounipolar trigeminal ganglion cells after injection of FB-solution into the whisker pad (see above). Following perfusion fixation (4 % paraformaldehyde), the

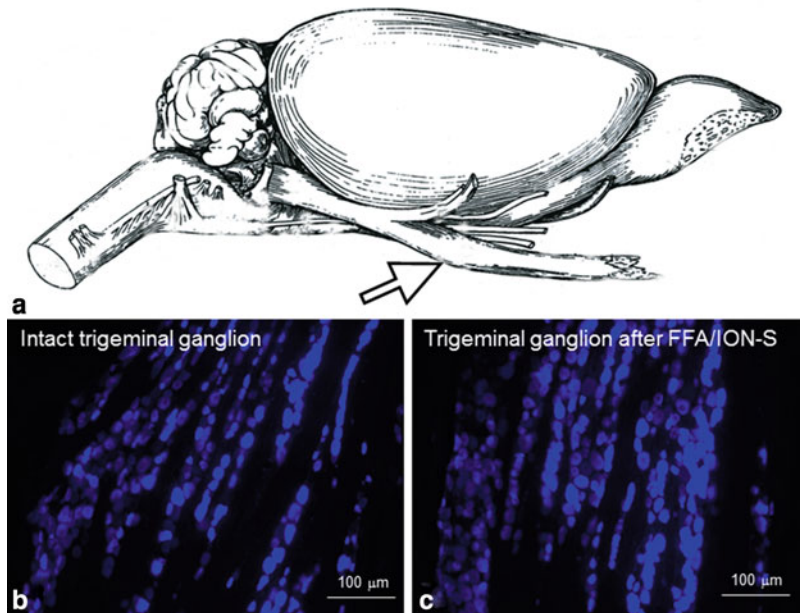


**Fig. 2.6** (a) Schematic drawing of the trigeminal ganglion (*arrow*), adapted from Greene (1935). (b, c) Retrogradely FB-labeled pseudounipolar sensory neurons in an intact trigeminal ganglion (b) and in a trigeminal ganglion 4 months after FFA + ION-S only (c). No major differences in the amount and distribution pattern of retrogradely labeled cells are evident. 30-µm-thick cryosections. Scale bar indicates 100 µm

trigeminal ganglia were dissected free (Fig. 2.6a), cryoprotected in 30 % sucrose, and cut into 30 thick longitudinal sections which were observed and photographed using the “ultraviolet” filter (set 01, Carl Zeiss).

Since the trigeminal ganglion spans 35–39 sections of 30-µm thickness, every third section was analyzed according to the fractionator selection strategy to determine the total neuron numbers with dendrites projecting into the whisker pad. All retrogradely labeled perikarya with a visible nucleus were counted on the operated and intact sides. Counting was performed blindly with respect to treatment.

### 2.1.11 Statistics

All data were analyzed using one-way ANOVA with post hoc Tukey’s test and significance level of  $p < 0.05$ . Statistica 6.0 software (StatSoft, Tulsa, OK, USA) was used for analysis.

## **2.2 Second Major Set: Intensive Indirect Stimulation of the Trigeminal Afferents After Facial Nerve Surgery by Excision of the Contralateral Infraorbital Nerve**

### **2.2.1 *Experiments to Determine the Degree of Collateral Axonal Branching by Application of Fluorescent Dyes on the Transected Superior and Inferior Buccolabial Rami of the Buccal Facial Branch***

#### **2.2.1.1 Animal Groups and Overview of the Specific Experiments**

Seventy rats were divided into seven groups (numbered 1–4 and 2a–4a). Group 1 (10 rats) served as unoperated control.

In groups 1–4, two animals served for electrophysiological measurements and were allowed to survive till 56 days post operation (DPO). The animals of groups 2–4 (each of 14 rats) were used for comparative assessment of axonal regrowth and branching by means of retrograde neuronal labeling. All rats were subjected to identical transection and suture of the right buccal branch of the facial nerve (buccal–buccal anastomosis, BBA). The rats of group 3 underwent BBA plus excision of the ipsilateral (right) ION and those of group 4 BBA plus excision of the contralateral (left) ION. The postoperative survival time was 28 days post surgery and 33–35 days post retrograde labeling. The timecourse was selected on the basis of behavioral observations showing partial restoration of vibrissae rhythmic whisking in some experimental groups during this period.

The animals of groups 2a–4a served to estimate the retraction of axonal branches (pruning or elimination of branches). All rats in groups 2a–4a (each of 6 rats) underwent BBA. The rats of group 3a underwent BBA plus excision of the ipsilateral (right) ION and those of groups 4a BBA plus excision of the contralateral (left) ION (ION-ex). The postoperative survival time was 112 days post surgery and 116–117 days post retrograde labeling.

#### **2.2.1.2 Surgery**

*Buccal–Buccal Anastomosis (BBA).* All operations were carried out under an operating microscope by trained microsurgeons. After intraperitoneal injection of ketamine plus xylazine (100 mg Ketanest<sup>®</sup> plus 5 mg Rompun<sup>®</sup> per kg body weight), the buccal branch of the facial nerve was exposed, transected, and immediately sutured with one epineural atraumatic 11–0 suture (Ethicon, Braunschweig, Germany). Since one experimental set of the present study (group C) focused on the accuracy of post-transectional reinnervation by the buccal branch of the facial nerve, we had to eliminate any additional innervation to the whisker pad muscles by the marginal mandibular branch (Semba and Egger 1986). This is the reason why

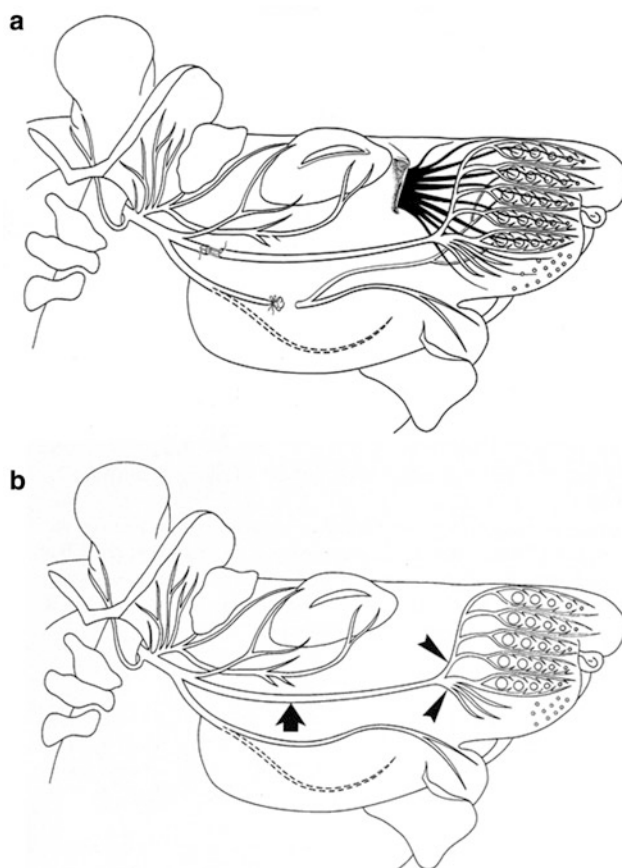


**Fig. 2.7** (a) Schematic drawing illustrating the close relationship between the peripheral fascicles of the facial nerve and those of ION (*in black*) and the sites of transection and suture in the buccal branch and of the transection and ligature of the marginal mandibular branch of the facial nerve. The cervical branch of the facial nerve is indicated by a *dotted line*. Adapted from Dörfel (1985) and Semba and Egger (1986). (b) Schematic drawing of all fascicles of the infratemporal portion of the rat facial nerve. *Large arrow* indicates the transection and suture site in the buccal branch of the facial nerve. Transection and tracer application sites in the superior and inferior buccolabial nerves are indicated by *arrowheads*

BBA was always accompanied by transection and proximal ligature (to prevent regeneration) of the marginal mandibular branch of the facial nerve (Fig. 2.7a).

*Excisions of the infraorbital nerve* were performed only in combination with FFA. Under ketamine/xylazine anesthesia, the infraorbital nerve ipsi- or contralateral to the side of FFA was transected at its exit from the infraorbital foramen, and all its peripheral fascicles were removed (resection paradigm; Fig. 2.1a, *upper arrow*).

The aim of this combined facial and trigeminal surgical treatment was to prove whether alterations in the trigeminal input to the axotomized electrophysiologically silent facial motoneurons might improve specificity of reinnervation. The rationale for this approach is derived from existence of direct ipsilateral and “crossed” connections between the trigeminal and facial nucleus (Kimura and Lyon 1972; Erzurumlu and Killackey 1979; Travers and Norgren 1983; Isokawa-Akesson and Komisaruk 1987).

### 2.2.1.3 Electrophysiological Measurements

In two additional rats of each experimental group, an electroneurography was performed on the right operated facial nerve 7, 28, and 56 DPO. In the control group (1), the measurements were done on day 0, and likewise 7, 28, and 56 days later. The right facial nerve was exposed and a bipolar recording needle electrode was inserted in the middle between the two dorsal vibrissal rows of the ipsilateral whisker pad. The flush-tip monopolar stimulator was placed under the buccal facial nerve directly proximal to the suture site (respectively 4 mm distal to the facial plexus in the two unoperated normal rats). Stimulation was performed for 0.2 ms at a supramaximal intensity of 8.0 mA. The recording analysis time was 50 ms with 10 to 1,000  $\mu$ V sensitivity and filters of 20 to 3,000 Hz. We measured the amplitude, that is, the peak-to-peak height of the main evoked electromyography waveform, excluding late waves. All measurements were repeated ten times. The data are described as means  $\pm$  SD. Group *t*-tests were used to evaluate the statistical significance of the differences between the experimental groups and the unoperated control group ( $p = 0.05$ ).

#### 2.2.1.4 Estimation of Axonal Regrowth and Branching: Application of Two Crystalline Tracers to Transected Superior and Inferior Buccolabial Nerves

It is well known that the post-transectional misdirection of axons may occur in three ways. *The first way* is that axons are simply misrouted along false endoneural tubes through wrong fascicles toward improper muscles (Esslen 1960; Thomander 1984; Aldskogius and Thomander 1986). *The second way* is that, in contrast with the precise target-directed pathfinding through single motor neurites during embryonic development (Liu and Westerfield 1990), several (but not one single) branches regrow from one transected axon (Shawe 1954; Esslen 1960; Brushart and Mesulam 1980; Ito and Kudo 1994; Baker et al. 1994). *The third way* of misdirection occurs through the intramuscular or terminal sprouting of axons within the target (Son et al. 1996).

In all 70 rats, we performed combined surgery on the facial nerve and ION and studied axonal regrowth peripherally to the transection site, but only within the distal stump of the buccal nerve and its bifurcation. Our aim was, by neglecting terminal

intramuscular sprouting (existing, but out of the scope of this chapter), to estimate both regrowth and branching of transected axons (Brown and Hopkins 1981; Jeng and Cogeshall 1984; Duncan and Baker 1987; Brushart 1993). This was quantitatively studied by neuron counts after application of the fluorescent retrograde tracers FluoroGold (FG; Fluorochrome Inc., Englewood, Colorado, 80155, USA) and DiI (1,1'-dioctadecyl-3,3,3',3'-tetramethylindocarbocyanine perchlorate, Molecular Probes, the Netherlands) to the superior and inferior buccolabial nerves (Fig. 2.7b).

1. In four anesthetized (ketamine/xylazine narcosis) animals of group 1 (unoperated control animals), the superior and inferior buccolabial nerves on the right side of the face were transected and labeled with crystals of DiI and FG, respectively. In the other four animals of group 1, the tracers were interchanged, that is, crystals of DiI were applied to the transected inferior and crystals of FG to the transected superior buccolabial nerve.
2. Identical bilateral labeling was done on day 56 (group 2) or day 112 (group 2a) after unilateral BBA.
3. Identical bilateral labeling was done on day 56 (group 3) or day 112 (group 3a) after unilateral BBA plus excision of the ipsilateral (right) ION.
4. Identical bilateral labeling was done on day 56 (group 4) or day 112 (group 4a) after unilateral BBA plus excision of the contralateral (left) ION.

### 2.2.1.5 Fixation, Tissue Processing, and Microscopy

*Fixation.* Five days after the double bilateral labeling (on day 61 or 117 after facial nerve surgery), all rats were transcardially perfused with 0.9 % NaCl in distilled water for 60 s followed by a fixation with 4 % paraformaldehyde in 0.1 M phosphate buffer (pH) 7.4 for 20 min under deep ether anesthesia. After removal of the whole brains, the brainstems were cut coronally in 50- $\mu$ m sections on a vibratome (FTB-vibracut; Plano, Marburg, Germany).

*Fluorescence Microscopy.* Vibratome sections were observed through filter set 01 of Carl Zeiss (excitation BP 365/12, emission LP 397), which allows recognition of FG-labeled motoneurons (appearing white). Observations through filter set 15 of Carl Zeiss (excitation BP 546/12, emission LP 590) revealed all motoneurons retrogradely labeled by DiI (appearing red). No fluorescence cross talk was observed between the two tracers used, that is, no DiI-labeled cells were visible through filter set 01 and no FG-labeled motoneurons could be observed using filter set 15. Employing a CCD video camera system (Optronics Engineering model DEI-470, Goleta, CA 93117, USA) combined with the image analyzing software Optimas 6.1 (Optimas Corporation, Bothell, Washington 98011, USA), the image observed with filter set 01 was superimposed on the image taken with filter set 15. The FG/DiI combined pictures of all unlesioned and lesioned facial nuclei in each of 30–33 vibratome sections per animal were saved in a color-coded TIFF format (Fig. 2.8a–f). For manual counting of retrogradely labeled motoneurons, the necessary TIFF file was simply loaded.

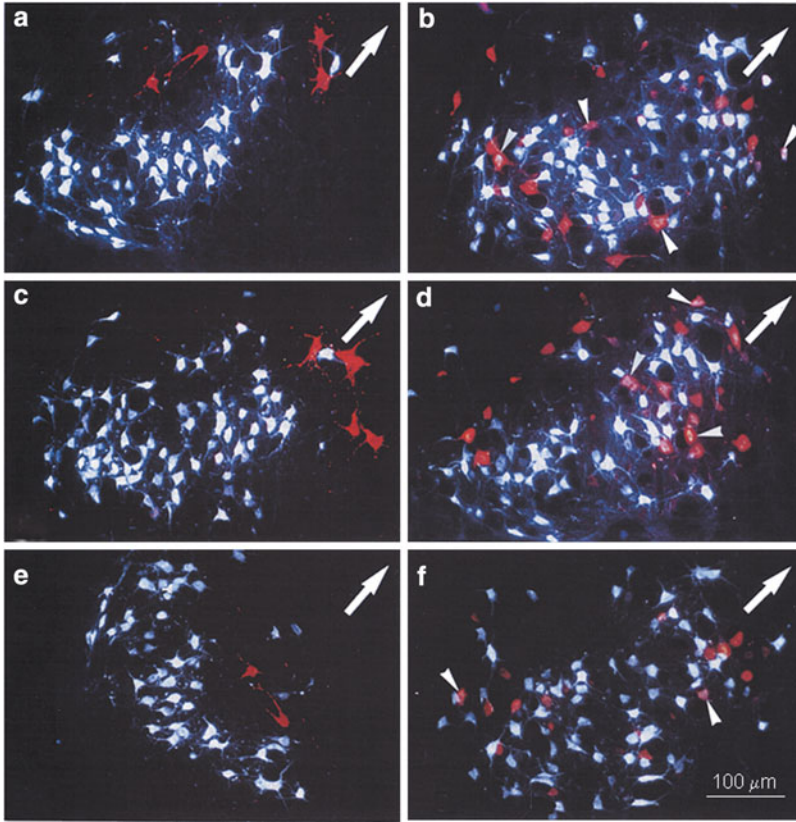


**Fig. 2.8** Rat brainstem 28 days after BBA. The dorsomedial portion of the facial nucleus is indicated by an *arrow*. (a) Contralateral unlesioned lateral facial subnucleus with preserved myotopic organization of the motoneurons whose axons project into the superior buccolabial nerve (retrogradely labeled in *white* by FluoroGold) and into the inferior buccolabial nerve (labeled in *red* by DiI). Whereas most FG-labeled motoneurons are localized in the ventrolateral portion, those labeled with DiI are in the dorsomedial part of the subnucleus. (b) Lesioned lateral facial subnucleus after BBA and application of FG to the superior and DiI to the inferior buccolabial nerve. Note the complete lack of myotopic organization: the FG-labeled (*white*), DiI-labeled (*red*), and DiI + FG-labeled (*arrowheads*) motoneurons are scattered throughout the whole lateral facial subnucleus. (c, d) Rat brainstem 28 days after BBA plus excision of the ipsilateral ION. Contralateral unlesioned lateral facial subnucleus with myotopic organization (c); Lesioned facial subnucleus 28 days after BBA plus excision of the ipsilateral ION (d). (e, f) Rat brainstem 28 days after BBA plus excision of the contralateral ION. Contralateral unlesioned lateral facial subnucleus with myotopic distribution of the motoneurons (e); lateral facial subnucleus 28 days after BBA plus excision of the contralateral ION (f). 50- $\mu$ m vibratome sections. Scale bar indicates 100  $\mu$ m

### 2.2.1.6 Quantitative Estimates

Single postoperative retrograde labeling of facial motoneurons with HRP injected into the whisker pad has shown that the reinnervation of the whisker pad muscles after transection and suture of the main trunk of the facial nerve can be studied in a

qualitative and in a quantitative aspect (Thomander 1984; Aldskogius and Thomander 1986; Angelov et al. 1993, 1996). The qualitative aspect is represented by the complete lack of myotopic organization: HRP-labeled motoneurons are scattered throughout the whole facial nucleus. This loss of myotopic organization in the facial nucleus following transection of the peripheral nerve is a direct morphological proof for the occurrence of “misdirected reinnervation” (termed also “misdirected resprouting,” “excessive reinnervation,” “aberrant reinnervation,” “aberrant regeneration,” or “misdirected regrowth of axons”). The quantitative aspect of misdirected reinnervation we called hyperinnervation, that is, our counts of HRP-labeled cells, showed that, following facial nerve surgery, there were up to 60 % more motoneurons projecting into the whisker pad muscles than under normal conditions (Angelov et al. 1996). This is why in the present report we also evaluated the reinnervation in a quantitative manner.

*Counting.* Employing the fractionator principle (Gundersen 1986), all retrogradely labeled motoneurons with visible cell nucleus in the 50- $\mu$ m-thick sections were counted in every third section through the facial nucleus on the operated and on the unoperated side (Guntinas-Lichius et al. 1993; Guntinas-Lichius and Neiss 1996).

### 2.2.1.7 Statistics

All data were analyzed as described in Sect. 2.1.11.

## 2.2.2 *Experiments to Determine the Accuracy of Reinnervation by Means of Intramuscular Injections of Fluorescent Dyes*

Sixty-one rats were used for two types of experiments:

1. Counts after retrograde labeling of facial motoneurons (41 rats)
2. Electrophysiological evaluations (20 rats)

The 41 rats in the anatomical studies were divided into four major groups:

*Control Group of 14 Rats.* Four rats received 1 % FluoroGold (FG) in the right whisker pad and 1 % Fast Blue (FB) in the left whisker pad. Another four rats received the same injection of FB in the right whisker pad and FG in the left whisker pad. These experiments established whether both tracers had similar efficiency in retrograde neuron labeling. Six other rats received 1 % FG in the right whisker pad, and 56 days later, 1 % FB was injected in the same site. These experiments tested whether the sequential injection of FG and FB in identical muscles can provide a reliable distinction between the FG-, the FB-, and the FG + FB-labeled neurons.

*Group FFA.* All nine animals received a bilateral intramuscular injection of FG. After 10 days they underwent unilateral FFA. After 56 days, a bilateral postoperative labeling with FB was performed at the site of the earlier FG-injection. The aim

of this postoperative labeling was not only to depict the motoneurons projecting into the selected muscles after surgery but to compare their location and number with those of the original innervation pool, which were permanently labeled by the nondegradable tracer FG.

*Group FFA Plus Excision of the Ipsilateral ION.* All 9 rats underwent identical preoperative labeling with FG. The postoperative labeling with FB was done 56 days after FFA and excision of the ipsilateral infraorbital nerve (ION, ipsi-ION-ex).

*Group FFA Plus Excision of the Contralateral (Left) Ion.* All nine rats underwent preoperative labeling with FG and postoperative injection with FB 56 days after FFA and excision of the contralateral ION (contra-ION-ex).

### 2.2.2.1 Preoperative FG-labeling of the Original Motoneuronal Pool

FG was always injected bilaterally. Because we intended to compare the number of retrogradely labeled motoneurons from different animals, great care was taken to ensure identical conditions of injection in all animals. Under diethylether anesthesia, 1 mg FG or 1 mg FB dissolved in 100  $\mu$ l distilled water containing 2 % dimethyl sulfoxide (DMSO) was injected in the whisker pad muscles at identical sites, at the midpoint between the two dorsal vibrissal rows (Arvidsson 1982). After 10 days, retrograde transport to the facial motoneurons was complete and the rats underwent surgery.

### 2.2.2.2 Surgery

All surgical operations were performed under an operating microscope. From earlier investigations of the post-transectional misdirection of *axons* projecting into the buccal branch of the facial nerve (Angelov et al. 1999), we learned to ignore the additional innervation of the whisker pad muscles by the marginal mandibular branch (Semba and Egger 1986). In the present study, we focused on the accuracy of *muscle* reinnervation by the buccal branch of the facial nerve, so we had to eliminate additional innervation to the whisker pad muscles. This is why, in all three experimental groups, FFA was always accompanied by transection and proximal ligation (to prevent regeneration) of the marginal mandibular branch of the facial nerve (Fig. 2.7a).

*Facial-facial anastomosis (FFA)* was performed as already described in Sect. 2.1.2.

*Excisions of the ipsilateral or contralateral ION* were performed only in combination with FFA. Under ketamine/xylazine anesthesia, the ION was transected at its exit from the infraorbital foramen, and all its peripheral fascicles were removed (resection paradigm).

### 2.2.2.3 Postoperative Retrograde Labeling of Regenerated Motoneurons

Twenty-eight days post operation, all 27 rats of groups FFA, FFA + ipsi-ION-ex, and FFA + contra-ION-ex received bilateral injections of 1 % FB (1 mg FB in 100 µl distilled water with 2 % DMSO) into the whisker pad musculature, exactly at the same site of the earlier FG-injection.

### 2.2.2.4 Fixation and Tissue Processing

Ten days after the postoperative bilateral labeling, all rats were transcardially perfused with 0.9 % NaCl in distilled water for 60 s followed by a fixation with 4 % paraformaldehyde in 0.1 M phosphate buffer (pH 7.4) for 20 min under deep ether anesthesia. After removal of the whole brains, the brainstems were cut coronally in 50-µm sections on a vibratome.

### 2.2.2.5 Fluorescence Microscopy

Using standard procedures, FG and FB are both simultaneously visualized with the same UV epifluorescence excitation filter (Zeiss, filter set 01). However, previous experiments have shown that the blue emission of FB obscured the white emission of FG resulting in far too low numbers of FG-labeled neurons. Thus, the quantitative analysis of FG + FB double labeling requires selective custom-made filter sets that exclude most fluorescence cross talk between FG and FB but also reduce sensitivity (Popratiloff et al. 2001). The filter sets used were FG-filter: HQ-Schmalband-filter set (no. F36-050; excitation D 369/40; beam splitter 400DCLP; barrier filter HQ 635/30) and FB-filter: bandpass-filter set (no. F31-000; excitation D 436/10; beam splitter 450 DCLP; barrier filter D470/40) both supplied by AHF Analysentechnik (Tübingen D-72005, Germany).

Employing a CCD video camera system (Optronics Engineering model DEI-470, Goleta, CA 93117, USA) combined with the image analyzing software Optimas 6.5. (Optimas Corporation, Bothell, Washington 98011, USA), separate images of the FG- and FB-retrogradely labeled facial motoneurons were created using these selective special filter sets. The generated masks of FG-labeled cells were superimposed over the FB-image for the unlesioned as well as for the lesioned facial nucleus. With this approach, all cells stained by FG and FB and double labeled by FG + FB could be readily identified and counted (Fig. 2.9c, f, i, l).

### 2.2.2.6 Quantitative Estimates

*Counting.* By applying the fractionator principle (Gundersen 1986), all retrogradely labeled motoneurons with visible cell nucleus in the 50-µm-thick sections were counted in every third section through the facial nucleus on the operated and

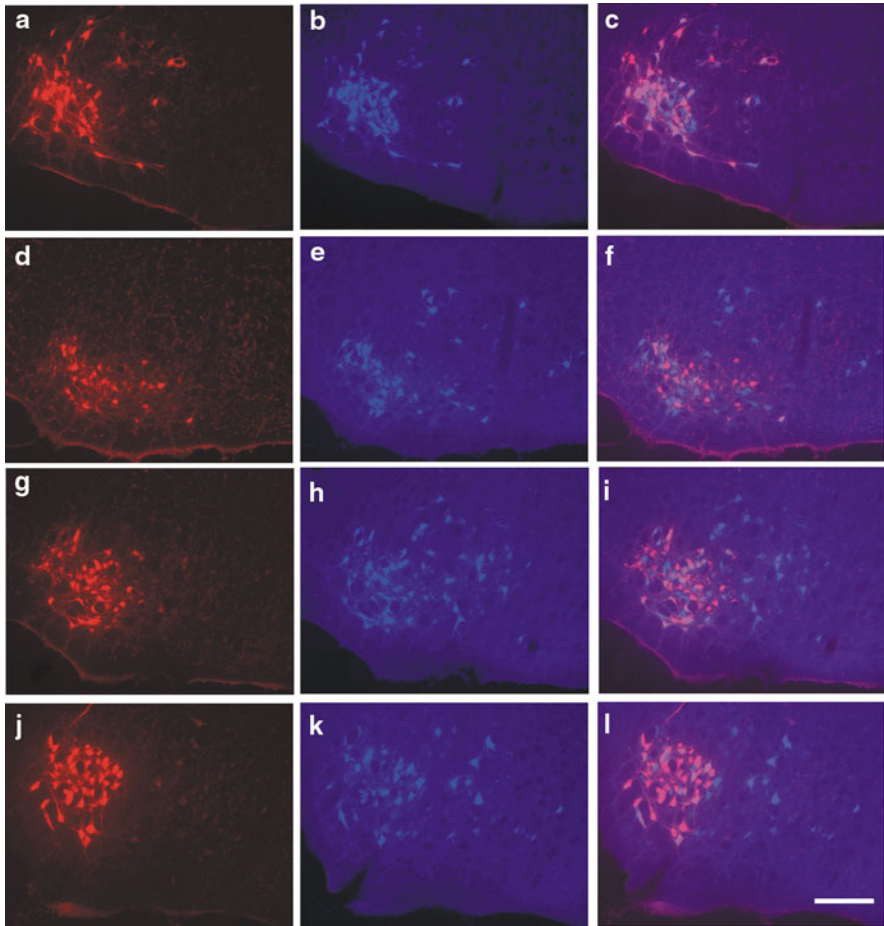


**Fig. 2.9** Rat brainstem 28 days after surgery on the buccal branch of the facial nerve. The lateral facial subnucleus, indicated by the preoperative FG-labeling is in the *left* part of each picture. All photographs in the *right* column were produced by double exposure. (a–b) Intact facial nucleus with preserved myotopic organization of the motoneurons. Employing the selective filters, we depicted all preoperatively FG-labeled (a) and all postoperatively FB-labeled (b) motoneurons. (c) In the intact facial nucleus, the portion of double-labeled (FG + FB, pink to bright purple in color) motoneurons is about 90 %. (d–f) Lesioned facial nucleus 28 days after BBA. Whereas all preoperatively FG-labeled motoneurons are localized in the lateral facial subnucleus (d), those labeled postoperatively with FB are observed also in the intermediate facial subnucleus (e). Our quantitative estimates show that only about 27 % of these FB-labeled motoneurons are double-labeled (f) and belong to the original motoneuronal pool of the whisker pad. (g–i) Lesioned facial nucleus of a rat 28 days after BBA plus excision of the ipsilateral ION. All preoperatively FG-labeled motoneurons are localized in the lateral facial subnucleus (g). The postoperatively FB-labeled motoneurons are found in the lateral and intermediate facial subnuclei (h). The double-exposure picture (i) is similar to that in (f) showing that about 32 % of the FB-labeled cells were also FG-labeled. (j–l) Lesioned facial nucleus of rat 28 days after BBA plus excision of the contralateral ION. All preoperatively FG-labeled motoneurons are localized in the lateral facial subnucleus (j) and some postoperatively FB-labeled cells are found in the intermediate facial subnucleus (k). Our counts show that after this type of combined surgery, the portion of the double-labeled motoneurons (l) increased significantly to 41 %. 50- $\mu$ m-thick vibratome sections. Scale bar indicates 100  $\mu$ m

unoperated side (Guntinas-Lichius et al. 1993, 2000; Guntinas-Lichius and Neiss 1996). All counts were performed by two observers, who were blind to the surgical procedure used on the rats.

### **2.2.2.7 Electrophysiological Measurements**

Ideally, the electrophysiological test was performed on the same rats that were injected with the retrotracers. This would, of course, provide the most accurate correlation between the two methods. Recently, however, Naumann et al. (2000) provided evidence for possible neurotoxic effects of FG in the medial septal nucleus/diagonal band complex about 6 weeks after retrograde labeling (Naumann et al. 2000). While the previous study focused on a different system and utilized a prolonged “post-labeling” period, we decided to avoid a potential risk of neurotoxicity by conducting the electrophysiological tests on rats that had not been injected with FG. Twenty rats were divided into four groups each consisting of five animals (1) intact rats (control group), (2) rats with unilateral FFA, (3) rats with FFA + ipsi-ION-ex, and (4) rats with FFA + contra-ION-ex. Recordings were performed on day 56 after surgery.

### **2.2.2.8 Stimulation and Recording**

Animals were deeply anesthetized with Nembutal (40 mg/kg body weight) and the body temperature was controlled during the entire recording session. Stimulation and recording were performed with a Neuropack 2 (Nihon Kohden Co., Japan) employing hooked subcutaneous silicon-coated silver wire electrodes (AG-10 T; Science Products GmbH, Germany). The silicone coating at the electrode tip was removed to allow adequate conduction.

Each electrode was inserted into a 20 G needle and hooked over its end. After insertion, the needle was gently retracted, leaving the electrode under the skin. In some animals, this procedure caused bleeding associated with a decline of the recorded signal. In these animals, all further experiments were canceled. The monitor was set to display 20 ms triggered by each stimulus. Recorded signals up to 100 Hz and above 10 kHz were cut off. Stimulation was applied using current mode.

Two stimulation electrodes were placed subcutaneously just in front of the anterior edge of the parotid gland, one above and one below the buccal branch of the facial nerve. The distance between both electrodes was approximately 5 mm. For recordings, a monopolar electrode was placed between the middle vibrissal rows C and D (Arvidsson 1982). Recordings were made with a negative active electrode. On all traces, depolarization of the muscles was indicated by a negative deflection.

To avoid interference from the excitation of other facial muscles, the reference or indifferent recording electrode was placed at a site as close as possible to the recorded ipsilateral vibrissal muscles. However, this procedure could not always be

performed perfectly. The innervation domain of the buccal branch, that is, the abundant piloerector muscles plus the levator labii superioris often received a thin communicating branch from the marginal mandibular branch of the facial nerve (Angelov et al. 1999; Semba and Egger 1986). In these cases, we had to attach the indifferent recording electrode proximally to the adjoining point of the communicating branch, which was distal from the whisker pad musculature. Animals were grounded with the aid of a subcutaneous stainless steel needle.

Providing valuable information about the extent of reinnervation and the speed of motor axon conduction, these experiments were designed to evaluate the compound muscle action potential (CMAP) generated by the whisker pad muscles after supramaximal stimulation of the buccal branch of the facial nerve. Once a maximal stimulus had been identified, the stimulation current was increased by 10 %. Usually 7–10 CMAPs were recorded.

### **2.2.2.9 Quantitative Estimates and Analysis**

Two parameters were taken into account: (1) the duration and (2) the amplitude of CMAP. Amplitude was expressed as difference between the maximum peak of CMAP and the baseline (in mV). Duration of CMAP was calculated by the distance between the points where the baseline was crossed by the rising and declining curves of the CMAP. For quantitative and qualitative purposes, the mean duration and amplitude of each experimental group (FFA, FFA + ipsi-ION-ex, FFA + contra-ION-ex) were compared to values obtained in unoperated control animals. The Kolmogorov–Smirnov one-sample test was used to test the normal distribution within the groups. All values are given as means  $\pm$  SD (standard deviation). Statistical comparisons of the CMAP measurements among the four groups were performed with ANOVA and followed by a Dunett T3 post hoc test. A *P* value of less than 0.01 was considered to indicate statistical significance. Unpaired *t*-test was used to prove whether the mean values for duration and amplitude of CMAPs were significantly different between each experimental group and the control group.

## **2.3 Third Major Set: Direct Stimulation of the Trigeminal and Facial Nerves After Facial Nerve Surgery by Massage of the Vibrissal Muscles**

### ***2.3.1 Animal Groups and Overview of Experiments***

One hundred and thirty-eight rats were used with two intact control groups and nine experimental groups (Table 2.5).

Group 1 consisted of 16 intact rats and group 2 of 16 experimental rats which were subjected to unilateral transection and suture of the right facial nerve

**Table 2.5** Experimental design flow chart

Group of animals	Video-based motion analysis of vibrissae motor performance	Degree of collateral axonal branching as estimated by triple retrograde labeling	Pattern of reinnervation of motor end plates in m. levator labii superioris
<b>Group 1: Intact animals (16 rats)</b>	16	8	8
Group 2: Animals with right FFA (16 rats)	16	8	8
Group 3: Animals with right FFA + EE (16 rats)	16	8	8
Group 4: Animals with right FFA + right MS (32 rats)	32	8	8
Group 5: Animals with right FFA + EE + right MS (16 rats)	16	8	8
Group 6: Animals with right FFA + left MS (6 rats)	6	—	6
Group 7: Animals with right FFA + handling (6 rats)	6	—	6
Group 8: Animals with right FFA + right ION-ex (6 rats)	6	—	6
Group 9: Animals with right FFA + right ION-ex + MS (6 rats)	6	—	6

Animal grouping and procedures, for example, facial–facial anastomosis (FFA), excision of the ipsilateral infraorbital nerve (ION-ex), dwelling in enriched environment (EE), and mechanical stimulation of the vibrissal muscles (MS). In groups 1–5, the animals that underwent video-based motion analysis were subsequently used for estimation of the degree of collateral axonal branching. In groups 6–9, the animals that were subjected to video-based motion analysis were thereafter used for establishing the pattern of motor end plates reinnervation

(facial–facial anastomosis, FFA) and were allowed to survive for 2 months. In both groups, all rats were used to determine vibrissal motor performance during explorative whisking using video-based motion analysis (Table 2.6). Thereafter, half of the animals were used to establish the degree of collateral axonal branching ipsilaterally by means of retrograde neuronal labeling (Table 2.7). Part of the results obtained for group 1 and 2 have already been published (Guntinas-Lichius et al. 2005b). The remaining eight rats in both groups were used to determine the proportion of mono- and polyinnervated motor end plates (Table 2.8) in the ipsilateral levator labii superioris muscle by means of immunocytochemistry for neuronal class III  $\beta$ -tubulin and histochemistry with alpha-bungarotoxin (see below).

**Table 2.6** Recovery of vibrissae function after facial nerve lesion in rats

Group of animals	Frequency (in Hz)	Angle at maximal protraction (in degrees)	Amplitude (in degrees)	Angular velocity during protraction (in degrees/s)
1. Intact	7.0 ± 0.8	62.0 ± 13.2 <sup>a</sup>	57 ± 13 <sup>a</sup>	1,238 ± 503 <sup>a</sup>
2. <i>Right FFA</i>	6.3 ± 0.5	91 ± 12 <sup>b</sup>	19 ± 6 <sup>b</sup>	135 ± 54 <sup>b</sup>
3. Right FFA + EE	6.8 ± 0.9	76 ± 6 <sup>a</sup>	26 ± 5 <sup>b</sup>	490 ± 187 <sup>b</sup>
4a. Right FFA + right MS for 1 min	6.5 ± 0.5	89 ± 6.2	13 ± 4	175 ± 68
	6.8 ± 0.9	91 ± 10	14 ± 7	159 ± 127
4b. Right FFA + right MS for 2 min	6.6 ± 0.5	66 ± 15 <sup>a</sup>	51 ± 19 <sup>a</sup>	1,019 ± 408 <sup>a</sup>
	6.8 ± 0.8	70 ± 11 <sup>a</sup>	36 ± 18 <sup>a</sup>	781 ± 329 <sup>a</sup>
4c. Right FFA + right MS for 5 min				
4d. Right FFA + right MS for 10 min				
5. Right FFA + EE + right MS	7.8 ± 2.3	65 ± 16 <sup>a</sup>	55 ± 20 <sup>a</sup>	1,124 ± 358 <sup>a</sup>
6. Right FFA + left MS	6.7 ± 1.0	94 ± 9.5 <sup>b</sup>	20 ± 9.5 <sup>b</sup>	368 ± 118 <sup>b</sup>
7. Right FFA + Handling	6.7 ± 0.8	104 ± 10.1 <sup>b</sup>	18 ± 3.4 <sup>b</sup>	316 ± 71 <sup>b</sup>
8. Right FFA + right ION-ex	6.0 ± 0.8	76 ± 10 <sup>b</sup>	22 ± 3.4 <sup>b</sup>	469 ± 400 <sup>b</sup>
9. Right FFA + right ION-ex + MS	6.0 ± 1.2	87 ± 18 <sup>b</sup>	14 ± 5.5 <sup>b</sup>	148 ± 68 <sup>b</sup>

Biometrics of vibrissae motor performance in intact rats (*Intact*), in rats after transection and suture of the right facial nerve only (*right FFA-only*), in rats subjected to FFA and postoperative dwelling in enriched environment (*right FFA + EE*), in rats that were subjected to FFA and postoperative mechanical stimulation of the right vibrissal muscles (*right FFA + right MS*), in rats subjected to combined treatment (*right FFA + EE + right MS*), in rats that were subjected to FFA and postoperative mechanical stimulation of the left vibrissal muscles (*right FFA + left MS*), in rats subjected to FFA and postoperative handling (*right FFA + handling*), and in rats subjected to excision of the ipsilateral infraorbital nerve (ION-ex). Groups 1–3 and 5 consisted of 8 animals, group 4 of 32 rats, and groups 6–9 of 6 animals. Shown are group mean values ± SD. Significant differences between group mean values (ANOVA and post hoc Tukey's test,  $p < 0.05$ )

<sup>a</sup>From FFA

<sup>b</sup>From Intact, FFA + MS, and FFA + EE + MS

In groups 3–7, rats underwent unilateral FFA plus subsequent treatments. The animals of group 3 (16 rats) received environmental stimulation for 2 months in an enriched environment (EE). The animals of group 4 (32 rats) received manual stimulation (MS) of the right whisker pad muscles, and the animals of group 5 (16 rats) experienced an enriched environment plus manual stimulation of the right whiskers (EE + MS). Vibrissal motor performance, the degree of axonal branching, and the patterns of motor end plate reinnervation were analyzed.

Groups 6 and 7 consisted of six rats each. Animals in group 6 received FFA on the right side and manual stimulation of the intact contralateral (left) whisker pad muscles. Rats in group 7 received no stimulation of the vibrissal muscles but were

Table 2.7 Projection pattern of facial motoneurons after facial nerve lesion in rats

Group of animals	Neurons projecting only into the zygomatic nerve ( <i>Dil-only</i> )		Neurons projecting into the zygomatic and buccal nerves ( <i>Dil</i> + <i>FG</i> )		Neurons projecting into the zygomatic and marginal mandibular nerves ( <i>Dil</i> + <i>FB</i> )		All Dil-labeled neurons projecting into the zygomatic nerve ( <i>Dil</i> , <i>Dil</i> + <i>FG</i> , <i>Dil</i> + <i>FB</i> )		Neurons projecting only into the buccal nerve ( <i>FG-only</i> )		Neurons projecting only into the marginal mandibular nerve ( <i>FB-only</i> )	
	Count	%	Count	%	Count	%	Count	%	Count	%	Count	%
<b>Intact<sup>a</sup></b>	364 ± 47	100 %	–	0 %	–	0 %	364 ± 47	100 %	1,441 ± 101	379 ± 94		
<b>FFA<sup>a</sup></b>	213 ± 53	30 %	239 ± 52 <sup>b</sup>	34 %	257 ± 56 <sup>b</sup>	36 %	709 ± 178 <sup>b</sup>	100 %	1,908 ± 289 <sup>b</sup>	1,488 ± 356 <sup>b</sup>		
<b>FFA + EE</b>	208 ± 164	45 %	140 ± 78 <sup>b</sup>	30 %	117 ± 76 <sup>b</sup>	25 %	465 ± 234	100 %	2,871 ± 268 <sup>b, c</sup>	2,484 ± 409 <sup>b, c</sup>		
<b>FFA + MS for 5 min daily</b>	276 ± 219	36 %	268 ± 149 <sup>b</sup>	35 %	211 ± 105 <sup>b</sup>	29 %	756 ± 251 <sup>b</sup>	100 %	3,162 ± 342 <sup>b, c</sup>	2,614 ± 184 <sup>b, c</sup>		
<b>FFA + EE + MS</b>	351 ± 178	43 %	286 ± 137 <sup>b, d</sup>	35 %	174 ± 113 <sup>b</sup>	12 %	810 ± 256 <sup>b</sup>	100 %	2,790 ± 432 <sup>b, c</sup>	1,986 ± 210 <sup>b, c, e</sup>		

Number of motoneurons with axons in the zygomatic, buccal, or marginal mandibular branches of the facial nerve of intact rats (*Intact*), in rats after transection and suture of the right facial nerve (*FFA-only*), in rats subjected to postoperative dwelling in enriched environment (*FFA + EE*), in rats that received postoperative manual stimulation of the vibrissal hairs (*FFA + MS*), and in rats subjected to combined treatment (*FFA + EE + MS*). The animals were studied 10 days after triple retrograde labeling performed 56 days post surgery. At least eight animals were studied per group. Shown are group mean values ± SD. Significant differences between group mean values (ANOVA and post hoc Tukey's test, *p* < 0.05)

<sup>a</sup>Values adapted from Guntinas-Lichius et al. (2005b)

<sup>b</sup>From Intact

<sup>c</sup>From FFA

<sup>d</sup>From FFA + EE

<sup>e</sup>From FFA + EE and FFA + MS

The percentage values below the absolute numbers in columns 2-5 indicate the portions of motoneurons projecting through the zygomatic nerve with branched (Dil + FG or Dil + FB, column 3 and 4) and unbranched axons (Dil-only, column 2)

**Table 2.8** Quality of target muscle reinnervation

Group of animals	Monoinnervated motor end plates (percent)	Polyinnervated motor end plates (percent)	Non-innervated motor end plates (percent)	Total number of motor end plates examined
1. Intact	100 ± 0	0	0	1,543 ± 132
2. <i>Right FFA</i>	45 ± 9.6	53 ± 10	2.6 ± 1.8	1,326 ± 413
3. Right FFA + EE	50 ± 15	41 ± 15	8.9 ± 5.0 <sup>a</sup>	1,411 ± 441
4 Right FFA + right MS (5 min daily)	69 ± 7.9 <sup>a, b</sup>	22 ± 5.1 <sup>a, b</sup>	9.6 ± 3.9 <sup>a</sup>	1,640 ± 338
5. Right FFA + EE + right MS	66 ± 11 <sup>a</sup>	31 ± 10 <sup>a</sup>	2.7 ± 2.0 <sup>c</sup>	1,345 ± 319
6. Right FFA + left MS	38 ± 7	60 ± 13	2.0 ± 1.6	1,237 ± 249
7. Right FFA + handling	39 ± 6	57 ± 12	5.0 ± 2.1	1,402 ± 235
8. Right FFA + right ION-ex	51 ± 8.6	43.3 ± 9.4	5.7 ± 2.8	1,495 ± 435
9. Right FFA + right ION-ex + MS	41 ± 6.1	50.7 ± 10	8.3 ± 3.6	1,579 ± 443

Reinnervation pattern of the levator labii superioris muscle (LLS) motor end plates in intact rats (*Intact*), in rats after transection and suture of the right facial nerve only (*right FFA-only*), in rats subjected to FFA and postoperative dwelling in enriched environment (right FFA + EE), in rats subjected to FFA and postoperative manual mechanical stimulation of the right vibrissal muscles (*right FFA + right MS*), in rats subjected to combined treatment (*right FFA + EE + right MS*), in rats subjected to FFA and postoperative mechanical stimulation of the left vibrissal muscles (*right FFA + left MS*), in rats subjected to FFA and postoperative handling (*right FFA + handling*), and in rats subjected to excision of the ipsilateral infraorbital nerve (ION-ex). Motor end plates were classified as monoinnervated, polyinnervated, or non-innervated according to the number of beta-tubulin-immunoreactive axons that crossed the boundaries of the end plate. Groups 1–5 consisted of 8 animals, groups 6–9 of 6 rats. Shown are group mean values ± SD. Significant differences between group mean values (ANOVA and post hoc Tukey’s test,  $p < 0.05$ )

<sup>a</sup>From FFA

<sup>b</sup>From FFA + EE

<sup>c</sup>From FFA + EE and FFA+MS

Values for intact rats are given as reference values and not included in the analysis

handled by the experimenter in exactly the same way as during MS except that MS was not used (“handling”). Estimation of vibrissal motor performance and patterns of motor end plate reinnervation were estimated 2 months after surgery.

In addition, we took a two-step approach to examine the role of trigeminal afferents (infraorbital nerve) which provide the sensory innervation to the vibrissal muscles (Jacquin et al. 1993; Munger and Renehan 1989; Rice et al. 1993). First, we tested the influence of the trigeminal sensory input on the process of motor recovery by extirpating one of its branches, the infraorbital nerve. The procedure ablates sensory input from the vibrissal muscle pads to facial motoneurons. For this experiment we used two additional groups (Nrr. 8 and 9), each consisting of six rats. In group 8 rats received FFA plus excision of the ipsilateral infraorbital nerve (ION-ex) (FFA + ION-ex). In group 9 rats received FFA plus ION-ex but followed by MS (FFA + ION-ex + MS).

Second, we estimated, using synaptophysin immunohistochemistry, the influence of manual stimulation on the afferent synaptic input to the facial nucleus in three groups of rats (Nrr. 10–12;  $n = 6$  in each), namely, intact animals, rats with FFA (FFA-only), and rats with FFA plus MS (FFA + MS). Groups 10–12 are not indicated in Tables 2.5–2.8.

### 2.3.2 Surgery

Transection and end-to-end suture of the right facial nerve (facial–facial anastomosis, FFA) was performed as described in Sect. 2.1.2.

*Excision of the ipsilateral infraorbital nerve* was performed only in combination with FFA as described in Sect. 2.2.1.2.

### 2.3.3 Standard Housing/Enriched Environment

After surgery, all animals were allowed to recover in individual cages for 24 h. Thereafter, rats from groups 2, 4, 6, and 7 were placed in *standard* cages (425 mm × 266 mm × 185 mm; polycarbonate (Tecniplast, Buguggiate, Italy)), each cage with two rats.

All 16 rats in group 3 were placed together in specifically designed cages (three cages sized 610 mm × 435 mm × 215 mm and connected in a row via polycarbonate tunnels, Tecniplast, Buguggiate, Italy) where they experienced group living and an enriched environment consisting of horizontal and inclining platforms and various toys (hanging robes, bridges, tunnels, climbing ladders, balls). Objects and toys were randomly circulated by removing some and adding others during the course of the experiment (cf. van Praag et al. 2000). All 16 rats of group 5 were treated in an identical way, but they received in addition mechanical stimulation of the vibrissal muscles (see below).

### ***2.3.4 Mechanical Stimulation of the Vibrissal Muscles***

Mechanical stimulation (both manual as well as environmental) was initiated 1 day after surgery. Rats were daily subjected to gentle rhythmic forward stroking of the right (groups 4 and 5) or left (group 6) vibrissae and whisker pad muscles (Fig. 2.10a,b) 5 days a week. Rats of groups 5 and 6 were manually stimulated for 5 min a day, and rats of group 4 were further distributed into four subgroups (4a, 4b, 4c, and 4d) that were stimulated daily for 1 min, 2 min, 5 min, and 10 min, respectively. The pattern of manual stimulation that we selected mimicked the natural active vibrissal movements during whisking, that is, active protraction and passive retraction (Welker 1964; Wineski 1985). Animals rapidly became accustomed to this procedure within 2–3 days and did not show any signs of stress such a freezing or trying to bite, weight loss, or lack of grooming; rather, animals readily cooperated.

### ***2.3.5 Handling of the Animals***

All six rats of group 7 were subjected to daily “handling.” Starting from the first day after FFA, animals were carefully taken by an investigator out of the cage and held as if they were to receive MS for 5 min (Fig. 2.10c). Thereafter, rats were put back in the cages.

### ***2.3.6 Analysis of Vibrissae Motor Performance During Exploration***

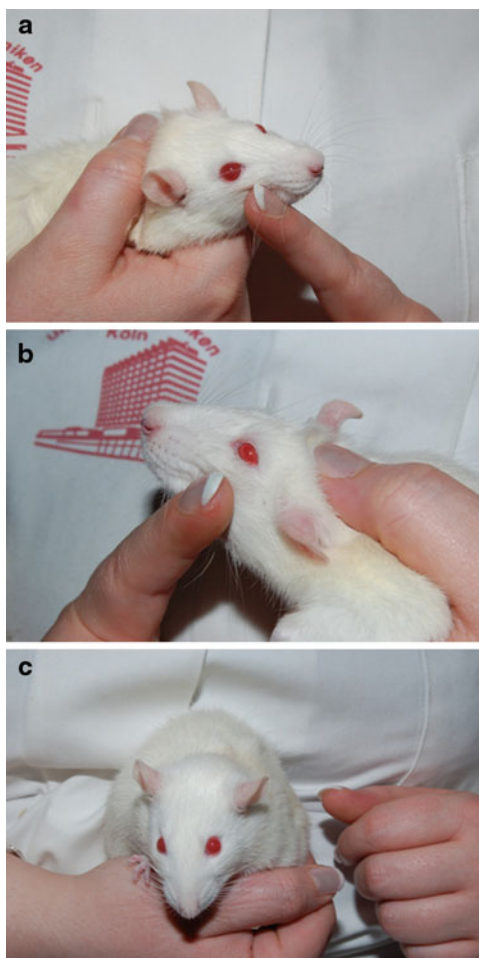
Video-based motion analysis of explorative vibrissal motor performance was performed as described previously in Sect. 2.1.6.

### ***2.3.7 Analysis of the Synaptic Input to the Facial Motoneurons***

To assess the synaptic input to the facial nucleus in intact rats and rats subjected to FFA with or without subsequent MS, we quantified levels of synaptophysin according to Calhoun et al. (1996) and Marqueste et al. (2006). Images were obtained on an epifluorescence microscope from sections stained with a highly diluted (1:4,000) anti-synaptophysin antibody. This protocol allowed us to obtain photo images in which, comparable to thin confocal optical sections, numerous puncta within the neuropil and around motoneuronal cell bodies in the facial nucleus were clearly discernible (cf. Fig. 2.3b–e).

**Fig. 2.10** Postoperative treatment of the rats.

(a) Manual mechanical stimulation of the right vibrissae and whisker pad muscles located ipsilateral to the nerve transection and suture (FFA). (b) Manual mechanical stimulation of the left vibrissae and whisker pad muscles located contralateral to FFA. (c) Handling of the animals



### 2.3.8 *Estimation of Axonal Branching by Triple Retrograde Labeling*

Earlier data after immunostaining of 50- $\mu\text{m}$ -thick vibratome sections for neuron-specific enolase (NSE) without retrograde labeling showed that the intact facial nucleus contained  $4,066 \pm 508$  NSE-immunoreactive perikarya (Angelov et al. 1994). Similar numbers were found after Nissl staining of paraffin sections ( $3,835 \pm 537$  facial neurons; Guntinas-Lichius et al. 1993). After retrograde labeling with horseradish peroxidase,  $3,973 \pm 187$  facial motoneurons were found (Angelov et al. 1993).

Subsequent work (Angelov et al. 1994) indicated no significant alterations in these values either at one ( $4,152 \pm 166$  facial neurons) or at 8 weeks after FFA ( $3,753 \pm 273$  facial neurons). Indeed, it has previously been established that axotomy of the facial nerve causes neuronal cell death only (1) if the rats under

study were newborn (Umemiya et al. 1993; Clatterbuck et al. 1994; Rossiter et al. 1996), (2) if the axotomy was performed by removal of the nerve at a length of approximately 1 cm which causes permanent deprivation from the target (Tetzlaff et al. 1988a, b), or (3) if the facial nerve axotomy was performed in mice, but not in rats (Raivich et al. 1998, 1999).

*Application of Fluorescence Tracers.* One day after videotaping, animals were anesthetized and crystals of DiI (1,1'-dioctadecyl-3,3,3',3'-tetramethylindocarbocyanine perchlorate, Molecular Probes, Leiden, the Netherlands), FluoroGold (FG; Fluorochrome Inc., Denver, Colorado, USA), and Fast Blue (FB; EMS-Chemie GmbH, Groß-Umstadt, Germany) were applied to the zygomatic, buccal, and marginal mandibular branches of the facial nerve, respectively, as described previously (Dohm et al. 2000). Crystals were left *in situ* for 30 min. Thereafter, the application sites were carefully rinsed and dried and the wound closed. Ten days later, animals were fixed by perfusion with 4 % formaldehyde in 0.1 M phosphate buffer (pH 7.4). Brainstems were sectioned in the frontal plane serially at 50- $\mu$ m thickness using a vibratome, mounted on slides, and dried at room temperature. The facial nucleus was visible in 32–36 serial sections, and analysis of every third section applying the fractionator principle (see below) allowed estimation of the total number of motoneurons with axons projecting into the ramus zygomaticus, ramus buccalis, and ramus marginalis mandibulae of intact rats (Fig. 2.11; Table 2.7).

*Fluorescence Microscopy.* Sections were observed with a Zeiss Axioskop 50 epifluorescence microscope (Zeiss, Oberkochen, Germany) using a custom-made bandpass-filter set combination (AHF Analysentechnik, Tübingen, Germany) which restricts the fluorescence cross talk between the tracers *ad maximum*. We used a CCD video camera system (Optronics DEI-470, Goleta, CA, USA) combined with the image analysis software Optimas 6.5. (Optimas Corporation, Bothell, Washington, USA) to create separate color images of retrogradely labeled facial motoneurons through the different filter sets. All images of DiI-labeled motoneurons were used to produce “DiI-masks” using Optimas: Frames were binarized and dilated and the outlines of each DiI-labeled cell depicted. Using the arithmetic options dialogue from the image menu, the masks were superimposed over the FB- or FG-picture. In this way, all cells stained by DiI<sub>only</sub>, FG<sub>only</sub>, FB<sub>only</sub>, as well as all those double stained by DiI + FG or DiI + FB could be readily identified and were manually counted on the computer screen (Dohm et al. 2000). This precise, though time-consuming, procedure allowed us to express the degree (index) of axonal branching in quantitative terms (sum of the percentages given in the third and fourth column in Table 2.7). In rats with an intact facial nerve trunk that had been subjected only to surgery for tracer application, the index of axonal branching was 0 %.

*Counting.* Employing the fractionator principle (Gundersen 1986), all retrogradely labeled motoneurons with visible cell nucleus in the 50- $\mu$ m-thick sections were counted in every third section through the facial nucleus on the operated and

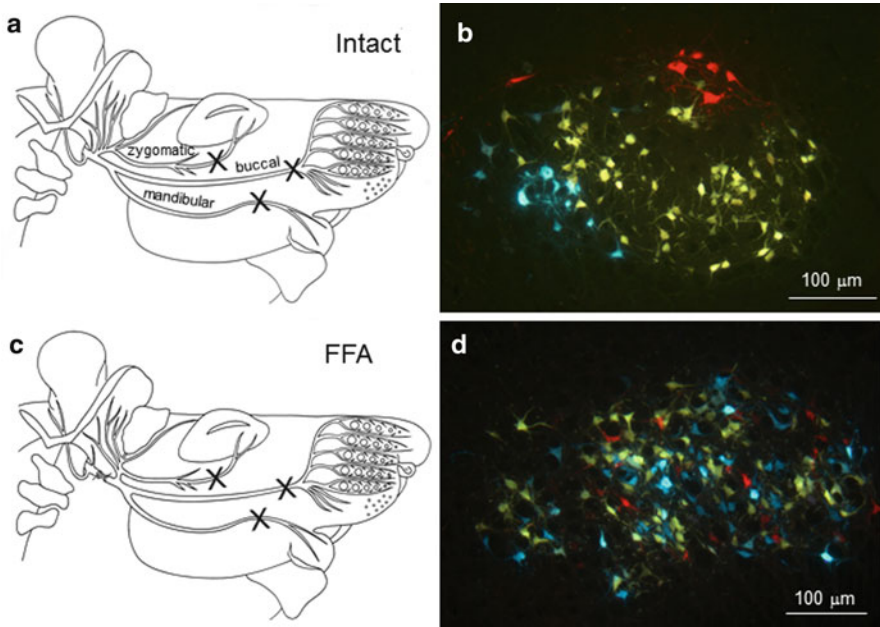


**Fig. 2.11** Myotopic organization of the facial nucleus and collateral axonal branching as estimated by the pattern of retrograde labeling. **(a, b)** In intact animals, simultaneous application of DiI (*red*), FG (*yellow*), and FB (*blue*) to the zygomatic, buccal, and mandibular nerve branches, respectively, labels distinct subnuclei with no overlap. **(c, d)** Two months after transection and suture of the facial nerve, the myotopic organization is lost irrespective whether the animals received ES or not. Adapted from Tomov et al. (2002)

on the intact side. Further details for this sampling technique have been described previously (Neiss et al. 1992; see also note on cell counting on page 98 in Valero-Cabre et al. 2004). Counting was performed blindly with respect to treatment.

### 2.3.9 Analysis of Target Muscle Reinnervation

Determination of the ratio between mono- and polyinnervated motor end plates was performed as described in Sect. 2.1.6.

### 2.3.10 Statistical Evaluation

All data were statistically analyzed as described in Sect. 2.1.11.

## **2.4 Fourth Major Set: Direct Stimulation of the Trigeminal and Facial Nerves After Facial Nerve Surgery by Application of Electric Current to the Vibrissal Muscles**

### ***2.4.1 Animal Groups and Overview of Experiments***

Ninety-six rats were divided into six groups each comprising 16 animals.

Group 1 consisted of intact rats and groups 2–6 of experimental rats that were subjected to unilateral transection and suture of the right facial nerve (facial–facial anastomosis, FFA; Fig. 2.12a). Animals in group 3 (resection) underwent removal of approximately 1 cm nerve length from the three main branches of the facial nerve (see below). Rats in group 4 (operated, but sham-stimulated, FFA + SS) had electrodes inserted in the denervated vibrissal muscles, but no electric current was applied. In group 5, the vibrissal muscles were subjected to ES (Fig. 2.12c).

Vibrissal motor performance during explorative whisking was analyzed in all rats using video-based motion analysis (Table 2.9). Following the functional analysis at 2 months after operation, half ( $n = 8$ ) of the animals in all groups were used to establish the degree of collateral axonal branching using triple retrograde neuronal labeling (Table 2.10). The remaining rats ( $n = 8$ ) were used to determine the proportion of mono- and polyinnervated motor end plates (Table 2.11) in the largest extrinsic ipsilateral vibrissal muscle, the levator labii superioris (LLS) muscle using immunocytochemistry for neuronal class III  $\beta$ -tubulin, AChE, and histochemistry for alpha-bungarotoxin (see below).

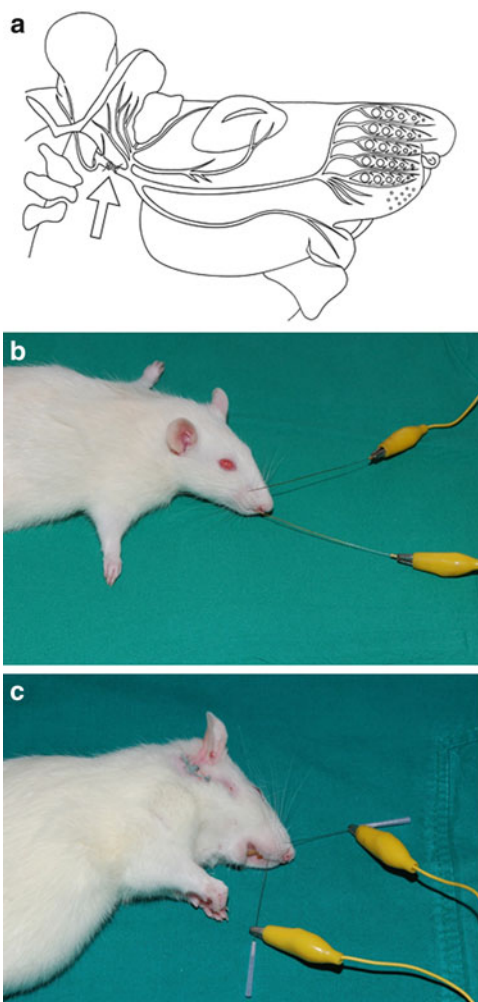
### ***2.4.2 Surgical Procedures***

All surgery was unilateral, performed under an operating microscope, and with surgical ketamine/xylazine anesthesia (100 mg Ketanest<sup>®</sup>, Parke–Davis/Pfizer, Karlsruhe, Germany, and 5 mg Rompun<sup>®</sup>, Bayer, Leverkusen, Germany, per kg body weight; i.p.).

*Transection and suture of the facial nerve* (facial–facial anastomosis, FFA) was performed as described in Sect. 2.1.2.

*Resection of the Facial Nerve.* The main trunk of the facial nerve was unilaterally mobilized at its emergence from the stylomastoid foramen, and pieces of 8–10 mm length were removed from the temporal, zygomatic, buccal, and upper and lower divisions of the marginal mandibular branch. This resection of the facial nerve is a very severe lesion in comparison to crush or transection of the nerve and delivers a permanent separation of the facial motoneurons from their target musculature.

**Fig. 2.12** (a) Schematic drawing of the infratemporal portion of the rat facial nerve. The site of transection and end-to-end suture of the facial nerve trunk, that is, facial-facial anastomosis (FFA) is indicated by an arrow. (b) Sham stimulation of rats: Acupuncture needle electrodes were inserted, but no current was applied to the electrodes. (c) Postoperative electrical stimulation of the vibrissal muscles. Adapted from Sinis et al. (2009)



### 2.4.3 Electrical Stimulation

Operated rats were subjected to electrical stimulation (ES) of the vibrissal muscles three times a week (Monday, Wednesday, and Friday) over 2 months starting on the first day after surgery. Electrical stimulation was delivered three times weekly since animals were required to be anesthetized. Under ketamine/xylazine anesthesia, two acupuncture needle electrodes were inserted toward LLS muscle, one along the uppermost vibrissal row A and the other in the lowest row D (Arvidsson 1982). The site of electrode placement close to the nose of the animal was thus somewhat distant (approximately 1 cm) to the location where the majority of LLS motor end plates are found, that is, at the borderline between the cheek and the whisker pad.

**Table 2.9** Recovery of vibrissae function after facial nerve injury in rats

Group of animals	Frequency (in Hz)	Angle at maximal protraction (in degrees)	Amplitude (in degrees)	Angular velocity during protraction (in degrees/s)
1. Intact <sup>a</sup>	7.0 ± 0.8	62 ± 13	57 ± 13	1,238 ± 503
2. FFA-only <sup>a</sup>	6.3 ± 0.5	91 ± 12	19 ± 6	135 ± 54
3. Resection	7.0 ± 0.8	102 ± 16	16 ± 5	323 ± 170
4. FFA + SS	5.8 ± 0.7	99 ± 11	16 ± 2.4	323 ± 81
5. FFA + ES	5.6 ± 1.1	106 ± 33	20 ± 8	211 ± 93
6. FFA + MS <sup>a</sup>	7.8 ± 2.3	65 ± 16	55 ± 20	1,124 ± 358

Biometrics of vibrissae motor performance in intact rats (*Intact*), in rats subjected to transection and suture of the facial nerve (*FFA-only*), in rats that underwent removal of 1 cm length from the main branches of the facial nerve (Resection paradigm), and in rats subjected to FFA plus postoperative sham stimulation (*FFA + SS*), postoperative electrical stimulation (*FFA + ES*), or postoperative mechanical stimulation of the whisker pad (*FFA + MS*). All groups consisted of 16 rats. Shown are group mean values ± SD. No significant differences between the control group 4 (*FFA + SS*) and the group with electrically stimulated rats (ANOVA and post hoc Dunnett's test,  $p < 0.05$ ) were detected

<sup>a</sup>Data adapted from Angelov et al. (2007)

The configuration thus allowed ES of the target muscles, the LLS, and part of the intrinsic vibrissal muscles close to the stimulating electrode, without the risk of direct damage to the motor end plates.

In all electrically stimulated rats ( $n = 16$ ), the threshold voltage required to elicit visible contractions of the whisker pad muscles and movements of the whiskers was initially determined by applying square 0.1 ms pulses at various voltage intensities using an isolated pulse stimulator (Master-8-cp, A.M.P.I., Jerusalem, Israel). The frequency selected (5 Hz) resembled the frequency of normal whisking. The muscles were stimulated for 5 min by applying square 0.1 ms pulses with suprathreshold amplitudes (typically 3.0–5.0 V; Fig. 2.12c). This stimulation was sufficient to depolarize intramuscular axons but not muscle fibers, innervated or denervated, in which action potentials can be elicited only upon much “stronger” stimulation, for example, pulses of 20-V amplitude and 5-ms duration for normal muscles and higher for denervated muscle fibers (Irintchev et al. 1990; Kern et al. 2002). Efficient muscle stimulation, especially that of denervated muscle fibers, requires delivery of high-voltage current pulses of long duration. This stimulation protocol was not approved by the animal welfare committee in Cologne because of the concern that “strong” stimulation might elicit trigeminal pain.

Control sham-stimulated rats were treated identically to rats subjected to ES except that no current was applied to the electrodes (Fig. 2.12b).

#### 2.4.4 Analysis of Vibrissal Motor Performance

Video-based motion analysis of vibrissal motor performance was performed as described previously in Sect. 2.1.6.

**Table 2.10** Projection pattern of facial motoneurons after facial nerve lesion in rats

Group of animals	Neurons projecting only into the zygomatic nerve ( <i>Dil-only</i> )	Neurons projecting into the zygomatic and buccal nerves ( <i>Dil + FG</i> )	Neurons projecting zygomatic and marginal mandibular nerves ( <i>Dil + FB</i> )	All Dil-labeled neurons projecting into the zygomatic nerve ( <i>Dil, Dil + FG, Dil + FB</i> )	Neurons projecting only into the buccal nerve ( <i>FG-only</i> )	Neurons projecting only into the marginal mandibular nerve ( <i>FB-only</i> )
<b>1. Intact<sup>a</sup></b>	364 ± 47 100 %	– 0 %	– 0 %	364 ± 47 100 %	1,441 ± 101	379 ± 94
<b>2. FFA-only<sup>a</sup></b>	213 ± 53 30 %	239 ± 52 34 %	257 ± 56 36 %	709 ± 178 100 %	1,908 ± 289	1,488 ± 356
<b>3. Resection</b>	0	0	0	0	0	0
4. FFA + SS	228 ± 165 43 %	159 ± 98 30 %	138 ± 79 27 %	525 ± 342 100 %	2,172 ± 256	1,881 ± 409
5. FFA + ES	321 ± 120 38 %	237 ± 102 28 %	276 ± 83 34 %	834 ± 305 100 %	2,254 ± 374	2,156 ± 262
6. FFA + MS <sup>1</sup>	276 ± 219 36 %	268 ± 149 35 %	211 ± 105 29 %	756 ± 251 100 %	3,162 ± 342	2,014 ± 184

Number of motoneurons with axons in the zygomatic, buccal, or marginal mandibular branches of the facial nerve in intact rats (*Intact*), in rats subjected to transection and suture of the facial nerve (*FFA-only*), in rats that underwent removal of 1 cm length from the main branches of the facial nerve (*Resection* paradigm), and in rats subjected to FFA plus postoperative sham stimulation (*FFA + SS*), postoperative electrical stimulation (*FFA + ES*), or postoperative mechanical stimulation of the whisker pad (*FFA + MS*). The percentage values below the absolute numbers in columns 2–5 indicate the portions of motoneurons projecting through the zygomatic nerve with branched (*Dil + FG or Dil + FB*, column 3 and 4) and unbranched axons (*Dil-only*, column 2). Animals were studied 10 days after triple retrograde labeling. At least eight animals were studied per group. Shown are group mean values ± SD. No significant differences between the control group 4 (*FFA + SS*) and the group with electrically stimulated rats (ANOVA and post hoc Dunnett's test,  $p < 0.05$ ) were detected. Data for groups 1, 2, and 6 are given as reference and are not included in the analysis

<sup>a</sup>Data adapted from Angelov et al. (2007)

**Table 2.11** Quality of target muscle reinnervation

Group of animals	Monoinnervated motor end plates (percent)	Polyinnervated motor end plates (percent)	Non-innervated motor end plates (percent)	Total number of motor end plates in LLS muscle
1. Intact rats <sup>a</sup>	100 ± 0	0	0	1,543 ± 132
2. FFA-only <sup>a</sup>	45 ± 9.6	53 ± 10	2.6 ± 1.8	1,326 ± 413
3. Resection	3.1 ± 0.6	1.6 ± 0.4	95 ± 22	416 ± 113
4. FFA + SS	49 ± 7.7	49 ± 9.4	2.4 ± 0.8	1,398 ± 415
5. FFA + ES	4.4 ± 1.8 <sup>b</sup>	5.5 ± 1.4 <sup>b</sup>	91 ± 25 <sup>b</sup>	346 ± 189 <sup>b</sup>
6. FFA + MS <sup>a</sup>	69 ± 7.9	22 ± 5.1	9.6 ± 3.9	1,640 ± 338

Innervation pattern of the levator labii superioris (LLS) muscle motor end plates in intact rats (Intact), in rats subjected to transection and suture of the facial nerve (*FFA-only*), in rats that underwent removal of 1 cm length from the main branches of the facial nerve (Resection paradigm), in rats subjected to FFA plus postoperative sham stimulation (*FFA + SS*), postoperative electrical stimulation (*FFA + ES*), or postoperative mechanical stimulation of the whisker pad (*FFA + MS*). At least eight animals were studied per group. Shown are group mean values ± SD. Data for groups 1–3 and 6 are given as reference and are not included in the analysis

<sup>a</sup>Data adapted from Angelov et al. (2007)

<sup>b</sup>Difference between groups 4 (*FFA + SS*) and 5 (*FFA + ES*) at 2 months after surgery (ANOVA and post hoc Dunnett's test,  $p < 0.05$ )

### 2.4.5 Estimation of Axonal Branching by Triple Retrograde Labeling

Application of fluorescence tracers, tissue preparation, microscopy, and evaluations were described in Sect. 2.3.7.

### 2.4.6 Analysis of Target Muscle Reinnervation

The ratio between mono- and polyinnervated motor end plates was estimated as described in Sect. 2.1.8.

### 2.4.7 Statistical Evaluation

Data were statistically analyzed as described in Sect. 2.1.11.

Stimulation of Trigeminal Afferents Improves Motor  
Recovery After Facial Nerve Injury  
Functional, Electrophysiological and Morphological  
Proofs

Skouras, E.; Pavlov, S.; Bendella, H.; Angelov, D.N.  
2013, XV, 110 p., Softcover  
ISBN: 978-3-642-33310-1